

THE ADAPTIVITY REFINES APPROXIMATE SOLUTIONS OF ILL-POSED PROBLEMS DUE TO THE RELAXATION PROPERTY

LARISA BEILINA* AND MICHAEL V. KLIBANOV** , * DEPARTMENT OF MATHEMATICAL SCIENCES ,
 CHALMERS UNIVERSITY OF TECHNOLOGY AND GOTHENBURG UNIVERSITY , SE-42196, GOTHENBURG,
 SWEDEN. , **DEPARTMENT OF MATHEMATICS AND STATISTICS , UNIVERSITY OF NORTH CAROLINA AT
 CHARLOTTE, , CHARLOTTE, NC 28223, USA. , AND E-MAILS: LARISA@CHALMERS.SE,
 MKLIBANV@UNCC.EDU

Abstract. Adaptive Finite Element Method (adaptivity) is known to be an effective numerical tool for some ill-posed problems. The key advantage of the adaptivity is the image improvement with local mesh refinements. A rigorous proof of this property is the central part of this paper. In terms of Coefficient Inverse Problems with single measurement data, the authors consider the adaptivity as the second stage of a two-stage numerical procedure. The first stage delivers a good approximation of the exact coefficient without an advanced knowledge of a small neighborhood of that coefficient. This is a necessary element for the adaptivity to start iterations from. Numerical results for the two-stage procedure are presented for both computationally simulated and experimental data.

AMS Subject Classification: 35L10, 35K10, 94A40

Key Words: Adaptive Finite Element Method, relaxation property, Ill-Posed problems, Coefficient Inverse Problem, numerical studies

1. Introduction. For the first time, the relaxation property for the Adaptive Finite Element Method (adaptivity) for a class of non-linear ill-posed problems was proved analytically in [16]. The relaxation property ensures that the adaptivity is worth to work with. In short, the relaxation is a rigorously derived estimate, which shows that the solution computed on a finer mesh is more accurate than the one computed on a coarser mesh. Unlike classical Well-Posed problems, this property is not automatic for Ill-Posed problems: because of the instability of the inversion in the latter case. The main results of the current paper is Theorem 5.2 (section 5), where a proof, simpler than the one of [16], is presented. Prior to [16] the relaxation was observed numerically, rather than analytically, in a number of publications about Coefficient Inverse Problem (CIPs), see, e.g. [1, 6, 7, 8, 9, 10, 13, 14, 15].

In most theorems of this paper (although not in all of them) we consider only the nonlinear finite dimensional case. The infinitely dimensional case would likely result in imposing the well known source representation condition, i.e. assuming that the solution belongs to the range of a certain compact operator. The latter cannot be effectively verified. On the other hand, since we are focused on applications of our theory to CIPs, then the work in a finite dimensional space is well justified by the fact that we actually work with finite elements, the number of which cannot be too large in any practical computation.

In our analytical derivations throughout the paper we assume that the noise level δ is sufficiently small. This is both a common and natural assumption in the theory of Ill-Posed problems, especially in the nonlinear case. Indeed, in principle one can hope to get an accurate solution only if the noise level is small. However, if the noise is large, then only a very special procedure, which is designed for a specific problem of interest, might or might not deliver an accurate solution. Those procedures cannot be described in the framework of Functional Analysis, since each such procedure highly depends on many specifics of a problem of interest. On the other hand, such a procedure took place for the second numerical example of this paper, which is for experimental data. And noise was quite large in this case: see comments in the beginning of Section 8.2. This confirms a commonly known observation that the theory is usually more pessimistic than numerical examples.

This paper summarizes recent results of the authors on the relaxation property for the adaptivity for Ill-Posed problems, see [11, 16, 33]. First, results are formulated in the Functional Analysis setting. Next, they are applied to a CIP for a hyperbolic PDE. Both formulations and proofs of almost all theorems are modified here, compared with above publications. It is shown in section 8 (Remark 8.2) that the relaxation property helps to work out the stopping criterion for mesh refinements. Theorems 5.3 and 5.4 as well as the numerical example of Test 1 were not published before.

The essence of the adaptivity consists in the minimization of the Tikhonov functional on a sequence

of locally refined meshes. It is important that due to local rather than global mesh refinements, the total number of finite elements is rather moderate. If this number would be very large, then the corresponding space of finite elements would effectively behave as an infinitely dimensional one. However, in the case of a moderate number of finite elements, this space effectively behaves as a finite dimensional one. Since all norms in finite dimensional spaces are equivalent, then we use the same norm in the Tikhonov regularization term as the one in the original space (except of Section 2.1). This is obviously more convenient for both analysis and numerical studies than the standard case of a stronger norm in this term [2, 11, 27, 45, 46]. Numerical results of the current and previous publications confirm the validity of this approach. Note that although the finite dimensional version of the original ill-posed problem might be well posed, at least formally, in the actuality it inherits the ill-posedness at certain extent. Thus, the use of the regularization term is still important for the stabilization.

Recall that a minimizer of the Tikhonov functional, if it exists, is called *regularized solution* of the corresponding equation [2, 11, 23, 27, 45, 46]. It is well known, however, that Tikhonov functionals for nonlinear Ill-Posed problems, such as, e.g. CIPs, suffer from the phenomenon of multiple local minima and ravines. Hence, many regularized solutions might exist. In addition, there is no guarantee that a gradient-like or a Newton-like method of minimizing such a functional would converge to the exact solution x^* , unless the first guess x_0 would not be sufficiently close to x^* . In other words, those are locally convergent methods, so as the adaptivity is. Therefore, the assumption in some theorems of this paper that the norm $\|x_0 - x^*\|$ is sufficiently small is a natural one, and the goal of the adaptivity is to refine x_0 .

Assuming that the norm $\|x_0 - x^*\|$ is sufficiently small, we estimate below the distance between a regularized solution and the one obtained after adaptive mesh refinements. Next, we estimate the distance between the latter solution and x^* . These are the so-called “*a posteriori* error estimates” (Theorems 5.2, 5.3, 6.4 and 6.5 below). This is a new element here. Indeed, in the past publications about the adaptivity for ill-posed problems, a posteriori error estimates were obtained only for either the Tikhonov functional or the Lagrangian, rather than for solutions themselves, see, e.g. [1, 4, 6, 7, 9, 10, 13, 14].

It follows from the above discussion that, prior to applying the adaptivity to a CIP, it is necessary to figure out at least one point in a small neighborhood of the correct solution. Hence, we have developed a two stage numerical procedure for some CIPs for a hyperbolic PDE. On the first stage, the so-called “approximately globally convergent method” [11, 12, 17, 32, 35, 37, 38] delivers the key ingredient of any locally convergent method: a good approximation x_0 for the exact solution x^* . On the second stage, the adaptivity uses this approximation as a starting point for a refinement [11, 13, 14, 15].

The adaptivity for an ill-posed problem, specifically for a CIP for a hyperbolic PDE, was first proposed in 2001 in [6]. Also, in 2001 a similar idea was proposed in [4], although an example of a CIP was not considered in [4]. In both these first publications the so-called “Galerkin orthogonality principle” was used quite essentially. The adaptivity was developed further in a number of publications, where it was applied to CIPs [3, 6, 7, 8, 9, 10]. A posteriori error estimates in an approximately globally convergent method was derived and an adaptive globally convergent method was developed at the first time in [1]. In [36] a posteriori error estimates was presented and an adaptive finite element method was applied for the solution of a Fredholm integral equation of a first kind. We also refer to [26] where the adaptivity was applied to a parameter identification problem. In a CIP an unknown coefficient of a PDE should be reconstructed using boundary measurements. In a parameter identification problem an unknown coefficient is reconstructed assuming that the solution of the corresponding PDE is given either everywhere inside of the domain of interest or on a grid inside of this domain. In the recent publication [40] the adaptivity was applied, for the first time, to the classical Cauchy problem for the Laplace equation and quite accurate images were obtained. Unlike other works on this topic, both lower and upper error estimates were obtained in [40].

In the sections 2-5 we use the apparatus of the Functional Analysis to address above items 1-4 for rather general ill-posed problems. In section 6 we deduce from sections 2-5 some results for a CIP for a hyperbolic PDE. In section 7 we present mesh refinement recommendations. In section 8 we present numerical results, including ones for real experimental data. In numerical studies of this paper we use the above mentioned two-stage numerical procedure.

2. Minimizing Sequence and a Regularized Solution Versus the First Guess. In this section we estimate the distances between terms of the minimizing sequence of the Tikhonov functional and the exact solution via the distance between the first guess and the exact solution. In the finite dimensional case the minimizing sequence is replaced with the regularized solution.

2.1. The infinitely dimensional case. Let B, B_1, B_2 be three Banach spaces. We denote norms in these spaces respectively as $\|\cdot\|, \|\cdot\|_1, \|\cdot\|_2$. As it is conventional in the theory of Ill-Posed problems, we assume that $B_1 \subseteq B, \|x\| \leq C \|x\|_1, \forall x \in B_1$ and $\overline{B_1} = B, C = \text{const.} > 0$, and the closure $\overline{B_1}$ is in the norm $\|\cdot\|$. Furthermore, we assume that any bounded set in B_1 is a compact set in B . Let $G \subseteq B_1$ be a set and \overline{G} be its closure in the norm $\|\cdot\|$. Let $F : \overline{G} \rightarrow B_2$ be a one-to-one operator, which is continuous in terms of norms $\|\cdot\|, \|\cdot\|_2$. Consider the equation

$$F(x) = y, x \in G. \quad (2.1)$$

As it is usually done in the regularization theory [2, 11, 23, 27, 45, 46], we assume that the right hand side of equation (2.1) is given with a small error $\delta \in (0, 1)$. We also assume that there exists an ‘‘ideal’’ exact solution x^* of (2.1) with the ‘‘ideal’’ exact data y^* (in principle, there might be several exact solutions). Thus, we assume that

$$F(x^*) = y^*, x^* \in G, \|y - y^*\|_2 \leq \delta. \quad (2.2)$$

Let $x_0 \in B_1$ be a first guess for the exact solution x^* . Usually one assumes that x_0 is located in a small neighborhood of x^* . Consider the Tikhonov functional

$$M_\alpha(x) = \frac{1}{2} \|F(x) - y\|_2^2 + \frac{\alpha}{2} \|x - x_0\|_1^2, x, x_0 \in G, \quad (2.3)$$

where $\alpha \in (0, 1)$ is the regularization parameter. We impose a rather conventional assumption that

$$\alpha = \alpha(\delta) = \delta^{2\mu}, \mu = \text{const.} \in (0, 1/2). \quad (2.4)$$

The second term in the right hand side of (2.3) is called ‘‘the Tikhonov regularization term’’. Let

$$m_\alpha = \inf_G M_\alpha(x). \quad (2.5)$$

Hence, there exists a minimizing sequence $\{x_n^\alpha\}_{n=1}^\infty \subset G$ such that $\lim_{n \rightarrow \infty} M_\alpha(x_n^\alpha) = m_\alpha$. By (2.2), (2.3) and (2.5)

$$m_\alpha \leq M_\alpha(x^*) < \delta^2 + \alpha \|x_0 - x^*\|_1^2. \quad (2.6)$$

Hence, there exists an integer $N = N(\delta, F) \geq 1$ such that $M_\alpha(x_n^{\alpha(\delta)}) < \delta^2 + \alpha \|x_0 - x^*\|_1, \forall n \geq N$. Hence, by (2.2)

$$\|x_n^{\alpha(\delta)}\|_1 \leq \sqrt{2} \left(\delta^{2(1-\mu)} + \|x_0 - x^*\|_1^2 \right)^{1/2} + \|x_0\|_1, \forall n \geq N(\delta, F). \quad (2.7)$$

Suppose that an *a priori* upper estimate of the distance between the first guess and the exact solution is given,

$$\|x_0 - x^*\|_1 \leq A, A = \text{const.} > 0, \quad (2.8)$$

where the number A is given. Then (2.7) implies that $\|x_n^{\alpha(\delta)}\|_1 \leq \sqrt{2}(A+1) + \|x_0\|_1$. Consider the set $P(x_0, A)$ defined as

$$P(x_0, A) = \left\{ x \in G : \|x\|_1 \leq \sqrt{2}(A+1) + \|x_0\|_1 \right\}. \quad (2.9)$$

Let $\overline{P} := \overline{P}(x_0, A)$ be its closure in terms of the norm $\|\cdot\|$. Hence, $\overline{P} \subseteq \overline{G}$. Since the set $P(x_0, A)$ is bounded in terms of the norm $\|\cdot\|_1$, then \overline{P} is a closed compact set in the space B . Consider the range $F(\overline{P}) \subset B_2$ of the operator F on the set \overline{P} . Since the operator $F : \overline{G} \rightarrow B_2$ is continuous in terms of norms $\|\cdot\|, \|\cdot\|_2$, then $F(\overline{P})$ is a closed compact set in B_2 . Furthermore, since F is one-to-one, then by the foundational theorem of Tikhonov [11, 27, 45, 46] the inverse operator $F^{-1} : F(\overline{P}) \rightarrow \overline{P}$ is continuous. Therefore, there exists the modulus of the continuity of the operator F^{-1} on the set $F(\overline{P})$. This means that there exists a function $\omega_F(z), z \in (0, \infty)$ such that

$$\omega_F(z) \geq 0, \omega_F(z_1) \leq \omega_F(z_2) \text{ if } z_1 \leq z_2, \lim_{z \rightarrow 0^+} \omega_F(z) = 0, \quad (2.10)$$

$$\|x_1 - x_2\| \leq \omega_F(\|F(x_1) - F(x_2)\|_2), \forall x_1, x_2 \in \overline{P}. \quad (2.11)$$

Theorem 2.1 compares the distance $\|x_0 - x^*\|_1$ with the distance between terms of the minimizing sequence and the exact solution x^* .

Theorem 2.1 (rate of convergence). *Let B, B_1, B_2 be Banach spaces, $G \subset B_1$ be a convex open set and $F : \overline{G} \rightarrow B_2$ be a one-to-one continuous operator in terms of norms $\|\cdot\|, \|\cdot\|_2$. Let conditions (2.2), (2.4), (2.5) and (2.8) be in place. Then for any number $\delta \in (0, 1)$ there exists an integer $N = N(\delta, F) \geq 1$ such that*

$$\|x_n^{\alpha(\delta)} - x^*\| \leq \omega_F\left(2\delta^\mu \sqrt{A+1}\right), \forall n \geq N(\delta, F). \quad (2.12)$$

Proof. Using (2.2) and (2.6), we obtain for $n \geq N(\delta, F)$

$$\begin{aligned} \|F(x_n^{\alpha(\delta)}) - F(x^*)\|_2 &= \|F(x_n^{\alpha(\delta)}) - y + y - F(x^*)\|_2 \\ &\leq \|F(x_n^{\alpha(\delta)}) - y\|_2 + \|y - y^*\|_2 \leq \left[2M_\alpha(x_n^{\alpha(\delta)})\right]^{1/2} + \delta \\ &\leq \left(\delta^2 + \delta^{2\mu} \|x_0 - x^*\|_1^2\right)^{1/2} + \delta \leq 2\delta^\mu \left(1 + \|x_0 - x^*\|_1^2\right)^{1/2} \leq 2\delta^\mu \sqrt{A+1}. \end{aligned} \quad (2.13)$$

By (2.6), (2.8) and (2.9) $x^* \in \overline{P}$. Therefore, (2.11) and (2.13) imply (2.12). \square

Theorem 2.1 estimates the distance $\|x_n^{\alpha(\delta)} - x^*\|$ via the distance $\|x_0 - x^*\|_1$ between the first guess and the exact solution for any $\delta \in (0, 1)$. Still, it is natural to ensure that the distance between terms of the minimizing sequence and the exact solution is strictly less than the distance between the first guess x_0 and the exact solution. This can be ensured only for sufficiently small values of the noise level δ . Although Corollary 2.1 has a similarity with the well known convergence theorem of the minimizing sequence for the Tikhonov functional (see, e.g. page 33 in [11]), still in that theorem only a subsequence converges rather than the entire sequence. Besides, estimate (2.14) is useful by its own right, and also the convergence rate (2.12), from which (2.14) is derived, seems to be new.

Corollary 2.1. *Let B, B_1, B_2 be Banach spaces, $G \subset B_1$ be a convex open set and $F : \overline{G} \rightarrow B_2$ be a one-to-one continuous operator in terms of norms $\|\cdot\|, \|\cdot\|_2$. Let conditions (2.2), (2.4), (2.5) and (2.8) be in place. Let $\xi \in (0, 1)$ be an arbitrary number. Assume first that $x_0 \neq x^*$. Then there exists a sufficiently small number $\delta_0 = \delta_0(F, A, \mu, \xi) \in (0, 1)$ such that*

$$\|x_n^{\alpha(\delta)} - x^*\| \leq \xi \|x_0 - x^*\|, \forall \delta \in (0, \delta_0), n \geq N(\delta, F). \quad (2.14)$$

In the case $x_0 = x^*$ (2.14) should be replaced with

$$\|x_n^{\alpha(\delta)} - x^*\| \leq \xi, \forall \delta \in (0, \delta_0), n \geq N(\delta, F). \quad (2.15)$$

In particular, if $\delta = 0$, then δ_0 should be replaced with a sufficiently small number $\alpha_0 \in (0, 1)$ and “ $\delta \in (0, \delta_0)$ ” should be replaced with $\alpha \in (0, \alpha_0)$.

Proof. First, let $x_0 \neq x^*$. By (2.10) there exists a sufficiently small number $\delta_0(F, A, \mu, \xi) \in (0, 1)$ such that $\omega_F(2\delta^\mu \sqrt{A+1}) \leq \xi \|x_0 - x^*\|, \forall \delta \in (0, \delta_0)$. Combining this with (2.12), we obtain (2.14).

Let now $x_0 = x^*$. Then again there exists a sufficiently small number $\delta_0(F, A, \mu, \xi) \in (0, 1)$ such that $\omega_F(2\delta^\mu \sqrt{A+1}) \leq \xi$. Combining this with (2.12), we obtain (2.15). \square

2.2. The finite dimensional case. Consider now the finite dimensional real valued Hilbert space. Compared with subsection 2.1, the main new point here is that the minimizing sequence is replaced with a minimizer, which exists. This case is of our main interest in the current paper because standard piecewise linear finite elements form a finite dimensional space. Unlike the above, we now use the same norm in the regularization term as in the original space. This is because all norms are equivalent in a finite dimensional space. Nevertheless, since the finite dimensional version of the original ill-posed problem “inherits” the ill-posedness, at certain extent, it is still important to use the regularization term for the stabilization.

Let H and H_2 be two real valued Hilbert spaces and $\dim H < \infty$. Norms and scalar products in these spaces denote respectively as $\|\cdot\|, (\cdot, \cdot), \|\cdot\|_2, (\cdot, \cdot)_2$. Let $G \subset H$ be an open bounded set and $F : \overline{G} \rightarrow H_2$ be a continuous operator. We again consider equations (2.1), (2.2), where $x^* \in G, y, y^* \in H_2$. The functional $M_\alpha(x)$ in (2.3) is now replaced with the functional $J_\alpha(x)$,

$$J_\alpha(x) = \frac{1}{2} \|F(x) - y\|_2^2 + \frac{\alpha}{2} \|x - x_0\|^2, x \in \overline{G}, x_0 \in G. \quad (2.16)$$

The following lemma follows immediately from Weierstrass theorem.

Lemma 2.1. *Let F be the operator defined above in this section. Then there exists a regularized solution $x_\alpha \in \overline{G}$,*

$$\inf_{\overline{G}} J_\alpha(x) = \min_{\overline{G}} J_\alpha(x) = J_\alpha(x_\alpha). \quad (2.17)$$

Although a similar result is valid for the case when the set G is unbounded, we do not formulate it here since we do not need it. The following theorem follows immediately from Theorem 2.1 and Corollary 2.1.

Theorem 2.2. *Let Hilbert spaces H, H_2 , the set $G \subset H$ and the operator $F : \overline{G} \rightarrow H_2$ be a one-to-one continuous operator. Let conditions (2.2), (2.8), (2.16) and (2.17) be in place. Then for any number $\delta \in (0, 1)$*

$$\|x_{\alpha(\delta)} - x^*\| \leq \omega_F(2\delta^\mu \sqrt{A+1}).$$

Let $\xi \in (0, 1)$ be an arbitrary constant. Then there exists a sufficiently small number $\delta_0 = \delta_0(F, A, \mu, \xi) \in (0, 1)$ such that for all $\delta \in (0, \delta_0)$

$$\|x_{\alpha(\delta)} - x^*\| \leq \begin{cases} \xi \|x_0 - x^*\|, & \text{if } x_0 \neq x^*, \\ \xi, & \text{if } x_0 = x^*. \end{cases}$$

In particular, if $\delta = 0$, then δ_0 should be replaced with a sufficiently small number $\alpha_0 \in (0, 1)$ and “ $\delta \in (0, \delta_0)$ ” should be replaced with $\alpha \in (0, \alpha_0)$.

3. The Local Strong Convexity of the Tikhonov Functional (2.16). In [43] the local strong convexity of the Tikhonov functional was established for the case when the underlying operator F has the second continuous Fréchet derivative and the source representation condition is in place. In this section we prove the local strong convexity of the Tikhonov functional (2.16) for the case when the operator F has the first continuous Fréchet derivative and the source representation condition is not imposed.

Let H and H_2 be two real valued Hilbert spaces. Let scalar products and norms in them be respectively $(\cdot, \cdot), \|\cdot\|$ and $(\cdot, \cdot)_2, \|\cdot\|_2$. Let $\mathcal{L}(H, H_2)$ be the the space of all bounded linear operators mapping H into H_2 and let $\|\cdot\|_{\mathcal{L}}$ be the norm in $\mathcal{L}(H, H_2)$. Although we do not assume here that H is finite dimensional, we still use the same norm $\|x - x_0\|$ in the regularization term in (2.16) as the one in the original space H , rather than a stronger norm as in (2.3). This is again because our true goal is to work in a finite

dimensional space of finite elements in the adaptivity (section 1). For any $a > 0$ and for any $x \in H$ denote $V_a(x) = \{z \in H : \|x - z\| < a\}$. First, we formulate the following well known theorem.

Theorem 3.1. [41]. *Let $G \subseteq H$ be a convex open set and $L : G \rightarrow \mathbb{R}$ be a functional. Suppose that this functional has the Fréchet derivative $L'(x) \in \mathcal{L}(H, \mathbb{R})$ for every point $x \in G$. Then the strong convexity of L on the set G with the strong convexity constant $\rho > 0$ is equivalent with the following condition*

$$(L'(x) - L'(z), x - z) \geq 2\rho \|x - z\|^2, \forall x, z \in G. \quad (3.1)$$

Theorem 3.2. *Let $G \subseteq H$ be a convex open set and $F : \overline{G} \rightarrow H_2$ be an operator. Let $x^* \in G$ be an exact solution of equation (2.1) with the exact data y^* . Let $V_1(x^*) \subset G$ and let (2.2) holds. Assume that for every $x \in V_1(x^*)$ the operator F has the Fréchet derivative $F'(x) \in \mathcal{L}(H, H_2)$. Suppose that this derivative is uniformly bounded and Lipschitz continuous in $V_1(x^*)$, i.e.*

$$\|F'(x)\|_{\mathcal{L}} \leq N_1, \forall x \in V_1(x^*), \quad (3.2)$$

$$\|F'(x) - F'(z)\|_{\mathcal{L}} \leq N_2 \|x - z\|, \forall x, z \in V_1(x^*), \quad (3.3)$$

where $N_1, N_2 = \text{const.} > 0$. Let

$$\alpha = \alpha(\delta) = \delta^{2\mu}, \quad \forall \delta \in (0, 1), \quad (3.4)$$

$$\mu = \text{const.} \in \left(0, \frac{1}{4}\right). \quad (3.5)$$

Then there exists a sufficiently small number $\delta_0 = \delta_0(N_1, N_2, \mu) \in (0, 1)$ such that for all $\delta \in (0, \delta_0)$ the functional $J_{\alpha(\delta)}(x)$ is strongly convex in the neighborhood $V_{\delta^{3\mu}}(x^*)$ of x^* with the strong convexity constant $\alpha/4$. In the noiseless case with $\delta = 0$ one should replace “ $\delta_0 = \delta_0(N_1, N_2, \mu) \in (0, 1)$ ” with $\alpha_0 = \alpha_0(N_1, N_2) \in (0, 1)$ to be sufficiently small and require that $\alpha \in (0, \alpha_0)$.

We refer to [11, 16] for the proof of Theorem 3.2 since it is space consuming. Consider now the finite dimensional case.

Theorem 3.3. *Let $\dim H < \infty, G \subset H$ be an open bounded convex set, and the rest of conditions of Theorem 3.2 holds. Let in (2.16) the first guess x_0 for the exact solution x^* be so accurate that*

$$\|x_0 - x^*\| < \frac{\delta^{3\mu}}{3}. \quad (3.6)$$

Then there exists a sufficiently small number $\delta_0 = \delta_0(N_1, N_2, \mu) \in (0, 1)$ such that for every $\delta \in (0, \delta_0)$ and for $\alpha = \alpha(\delta)$ satisfying (3.4) there exists unique regularized solution $x_{\alpha(\delta)}$ of equation (2.1) on the set G . Furthermore, $x_{\alpha(\delta)} \in V_{\delta^{3\mu}}(x^*)$. In addition, the gradient method of the minimization of the functional $J_{\alpha(\delta)}(x)$, which starts at x_0 , converges to $x_{\alpha(\delta)}$. Also, if the operator F is one-to-one on $V_1(x^*)$, then $x_{\alpha(\delta)} \in V_{\delta^{3\mu}/3}(x^*)$. In the noiseless case with $\delta = 0$ one should replace “ $\delta_0 = \delta_0(N_1, N_2, \mu) \in (0, 1)$ ” with $\alpha_0 = \alpha_0(N_1, N_2) \in (0, 1)$ to be sufficiently small and require that $\alpha \in (0, \alpha_0)$.

Proof. By Lemma 2.1 there exists a minimizer $x_{\alpha(\delta)} \in \overline{G}$ of the functional $J_{\alpha(\delta)}$. We have $J_{\alpha(\delta)}(x_{\alpha(\delta)}) \leq J_{\alpha(\delta)}(x^*)$. Also, $\|x_{\alpha(\delta)} - x_0\| \geq \|x_{\alpha(\delta)} - x^*\| - \|x_0 - x^*\|$. Hence, using (2.2), (2.16) and (3.6), we obtain that there exists a sufficiently small number $\delta_0 = \delta_0(N_1, N_2, \mu) \in (0, 1)$ such that for every $\delta \in (0, \delta_0)$

$$\|x_{\alpha(\delta)} - x^*\| \leq \frac{\delta}{\sqrt{\alpha}} + 2\|x^* - x_0\| < \delta^{1-\mu} + \frac{2}{3}\delta^{3\mu} = \frac{2}{3}\delta^{3\mu} \left(1 + \frac{3}{2}\delta^{1-4\mu}\right) < \frac{2}{3}\delta^{3\mu} \cdot \frac{3}{2} = \delta^{3\mu}.$$

Hence, $x_{\alpha(\delta)} \in V_{\delta^{3\mu}}(x^*)$. Since by Theorem 3.2 the functional J_{α} is strongly convex on the set $V_{\delta^{3\mu}}(x^*)$ and the minimizer $x_{\alpha(\delta)} \in V_{\delta^{3\mu}}(x^*)$, then this minimizer is unique. Furthermore, since by (3.6) the point $x_0 \in V_{\delta^{3\mu}}(x^*)$, then it is well known that the gradient method with its starting point at x_0 converges to $x_{\alpha(\delta)}$.

Let now the operator F be one-to-one. Let $\xi \in (0, 1)$ be an arbitrary number and $x_0 \neq x^*$. By Theorem 2.2 we can choose a smaller number $\delta_0 = \delta_0(N_1, N_2, \mu, \xi)$ such that

$$\|x_{\alpha(\delta)} - x^*\| \leq \xi \|x_0 - x^*\|, \forall \delta \in (0, \delta_0).$$

Hence, (3.6) implies that $x_{\alpha(\delta)} \in V_{\delta^{3\mu}/3}(x^*)$. If $x_0 = x^*$, then by Theorem 2.2 $\|x_{\alpha(\delta)} - x^*\| \leq \xi$. Choosing $\xi \in (0, \delta^{3\mu}/3)$, we again obtain that $x_{\alpha(\delta)} \in V_{\delta^{3\mu}/3}(x^*)$. The noiseless case is similar. \square

4. The Space of Finite Elements. To prove the relaxation property of the adaptivity, we need to introduce the space of finite elements. Let $\Omega \subset \mathbb{R}^n$, $n = 2, 3$ be a bounded domain. Consider a discretization of Ω by an unstructured mesh T using non-overlapping tetrahedral elements in \mathbb{R}^3 and triangles in \mathbb{R}^2 such that $T = K_1, \dots, K_l$, where l is the number of elements in Ω , and

$$D = \cup_{K \in T} K = K_1 \cup K_2 \dots \cup K_l.$$

We obtain a polygonal domain D and assume for brevity that $D = \Omega$. We associate with the triangulation T the mesh function $h = h(x)$ which is a piecewise-constant function such that

$$h(x) = h_K \quad \forall K \in T,$$

where h_K is the diameter of K which we define as the longest side of K . Following section 76.4 of [25], consider piecewise linear functions $\{e_j(x, T)\}_{j=1}^N \subset C(\overline{\Omega})$, which are called *test functions*. Functions $\{e_j(x, T)\}_{j=1}^N$ are linearly independent in Ω . Here, N is the global number of nodes in the mesh T . Let $\{N_i\}$ be the set of nodal points of triangle/tetrahedra K for all $K \in T$. Then

$$e_j(N_i, T) = \begin{cases} 1, & i = j, \\ 0, & i \neq j. \end{cases}$$

We introduce the finite element space V_h as

$$V_h = \{v(x) \in V : v \in C(\Omega), v|_K \in P_1(K) \forall K \in T\}, \quad (4.1)$$

where $P_1(K)$ denotes the set of piecewise-linear functions on K with

$$V = \{v(x) : v(x) \in L_2(\Omega)\}.$$

The finite dimensional finite element space V_h is constructed such that $V_h \subset V$.

Let r be the radius of the maximal circle/sphere inscribed in K . We impose the shape regularity assumption for all triangles/tetrahedra uniformly for all possible triangulations T which we consider. Specifically, we assume that

$$a_1 \leq h_K \leq ra_2, \quad a_1, a_2 = \text{const.} > 0, \quad \forall K \in T, \quad \forall T, \quad (4.2)$$

where numbers a_1, a_2 are independent on the triangulation T . Let $h_{\max}(T)$ and $h_{\min}(T)$ be respectively the maximal and minimal diameters of triangles/tetrahedra of the triangulation T . We assume evrywhere below that

$$\frac{h_{\min}(T)}{h_{\max}(T)} \leq c_T, \quad \forall T \quad (4.3)$$

for a certain positive constant c_T . Obviously, the number of all possible triangulations satisfying (4.2), (4.3) is finite. Thus, we introduce the following finite dimensional linear space H ,

$$H = \bigcup_T V_h(T), \quad \forall T \text{ satisfying (4.2), (4.3).}$$

Hence,

$$\dim H < \infty, H \subset (C(\overline{\Omega}) \cap H^1(\Omega)), \partial_{x_i} f \in L_\infty(\Omega), \forall f \in H. \quad (4.4)$$

In (4.4) " \subset " means the inclusion of sets. We equip H with the same inner product as the one in $L_2(\Omega)$. Denote (\cdot, \cdot) and $\|\cdot\|$ the inner product and the norm in H respectively, $\|f\|_H := \|f\|_{L_2(\Omega)} := \|f\|, \forall f \in H$. Everywhere below H is this space. We view the space H as an "ideal" space of very fine finite elements, which cannot be reached in practical computations. At the same time, all other spaces of finite elements we work with below are subspaces of H . In particular, this means that we assume without further mentioning that (4.2) and (4.3) are valid for all meshes considered below.

Keeping in mind the mesh refinement process in the adaptivity, we now explain how do we construct triangulations $\{T_n\}$ as well as corresponding subspaces $\{M_n\}$ of the space H which correspond to mesh refinements. Consider the first triangulation T_1 with rather coarse mesh. We set $M_1 := V_h(T_1) \subset H$. Suppose that the pair (T_n, M_n) is constructed after n mesh refinements and that the basis functions in the space M_n are $\{e_j(x, T_n)\}_{j=1}^{N_n}$. We now want to refine the mesh again. We define the pair (T_{n+1}, M_{n+1}) as follows. We refine the mesh in the standard manner as it is usually done when working with triangular/tetrahedron finite elements. When doing so, we keep (4.2). Hence, we obtain both the triangulation T_{n+1} and the corresponding test functions $\{e_j(x, T_{n+1})\}_{j=1}^{N_{n+1}}$. It is well known that test functions $\{e_j(x, T_n)\}_{j=1}^{N_n}$ are linearly dependent from new test functions $\{e_j(x, T_{n+1})\}_{j=1}^{N_{n+1}}$. Thus, we define the subspace M_{n+1} as

$$M_{n+1} := \text{Span} \left(\{e_j(x, T_{n+1})\}_{j=1}^{N_{n+1}} \right).$$

Therefore, we have obtained a finite set of linear subspaces $\{M_n\}_{n=1}^N$ of the space H . Each subspace M_n corresponds to the mesh refinement number $n, M_{n+1} \setminus M_n \neq \emptyset$ and

$$M_n \subset M_{n+1} \subset H, n \in [1, N-1].$$

Let I be the identity operator on H . For any subspace $M \subset H$, let $P_M : H \rightarrow M$ be the orthogonal projection operator of the space H onto its subspace M . Denote for brevity $P_n := P_{M_n}$. Let h_n be the maximal grid step size of T_n . Hence, $h_{n+1} \leq h_n$. Let f_n^I be the standard interpolant of the function $f \in H$ on triangles/tetrahedra of T_n , see section 76.4 of [25]. It can be easily derived from formula (76.3) of [25] that

$$\|f - f_n^I\| \leq K \|\nabla f\|_{L_\infty(\Omega)} h_n, \forall f \in H, \quad (4.5)$$

where $K = K(\Omega, r, a_1, a_2) = \text{const.} > 0$. Since $f_n^I \in H, \forall f \in H$, then by one of well known properties of orthogonal projection operators,

$$\|f - P_n f\| \leq \|f - f_n^I\|, \forall f \in H. \quad (4.6)$$

Hence, (4.5) and (4.6) imply that with a different constant $K = K(\Omega, r, a_1, a_2) > 0$

$$\|f - P_n f\| \leq K \|\nabla f\|_{L_\infty(\Omega)} h_n, \forall f \in H. \quad (4.7)$$

Since H is a finite dimensional space in which all norms are equivalent, it is convenient for us to rewrite (4.7) with a different constant $K = K(\Omega, r, a_1, a_2) > 0$ as

$$\|x - P_n x\| \leq K \|x\| h_n, \forall x \in H. \quad (4.8)$$

5. Relaxation. Since we sequentially minimize the Tikhonov functional on subspaces $\{M_n\}_{n=1}^N$ in the adaptivity procedure, then we need to establish first the existence of a minimizer on each of these subspaces. In this section the set G and the operator F are the same as in Theorem 3.3, and the functional $J_\alpha(x)$ is the

same as in (2.16). Theorem 5.1 ensures both existence and uniqueness of the minimizer of the functional J_α on each subspace of the space H , as long as the maximal grid step size of finite elements, which are involved in that subspace, is sufficiently small.

Theorem 5.1. *Let conditions of Theorem 3.3 hold. In particular, let the operator $F : \overline{G} \rightarrow H_2$ be one-to-one. Let $M \subseteq H$ be a subspace of H and let $V_{\delta^{3\mu}}(x^*) \cap M \neq \emptyset$. Assume that $\|x^*\| \leq B$, where the number $B > 0$ is known in advance. Suppose that the maximal grid step size \tilde{h} of finite elements of M be so small that*

$$\tilde{h} \leq \frac{\delta^{4\mu}}{5BN_2K}, \quad (5.1)$$

where K is the constant in (4.8). Furthermore, assume that the first guess x_0 for the exact solution x^* in the functional $J_{\alpha(\delta)}$ is so accurate that (3.6) is in place. Then there exists a sufficiently small number $\delta_0 = \delta_0(N_1, N_2, \mu) \in (0, 1)$ such that for every $\delta \in (0, \delta_0)$ there exists unique minimizer $x_{M, \alpha(\delta)} \in G \cap M$ of the functional J_α on the set $G \cap M$. Furthermore, $x_{M, \alpha(\delta)} \in V_{\delta^{3\mu}}(x^*) \cap M$. In addition, the functional $J_\alpha(x)$ is strongly convex on the set $V_{\delta^{3\mu}}(x^*) \cap M$ with the strong convexity constant $\alpha(\delta)/4$. Let $x_{\alpha(\delta)} \in V_{\delta^{3\mu}/3}(x^*)$ be the regularized solution of equation (2.1), which is guaranteed by Theorem 3.3. Then the following a posteriori error estimate holds

$$\|x_{M, \alpha(\delta)} - x_{\alpha(\delta)}\| \leq \frac{2}{\delta^{2\mu}} \|J'_\alpha(x_{M, \alpha(\delta)})\|.$$

Note that since in Theorem 5.1 $V_1(x^*) \subset G$ and $V_{\delta^{3\mu}}(x^*) \cap M \neq \emptyset$, then $G \cap M \neq \emptyset$. We do not prove this theorem here and refer instead to Theorem 4.9.2 of [11]; also see Theorem 3.2 of [16] for a similar result.

Theorem 5.2 (relaxation). *Let $M_n \subset H$ be the subspace obtained after n mesh refinements, as described in section 4. Let h_n be the maximal grid step size of the subspace M_n . Suppose that all conditions of Theorem 5.1 hold with the only exception that the subspace M is replaced with M_n and the inequality (5.1) is replaced with*

$$h_n \leq \frac{\delta^{4\mu}}{5BN_2K}. \quad (5.2)$$

Let $\delta \in (0, \delta_0)$, where the number $\delta_0 \in (0, 1)$ is defined in Theorem 5.1. Also, let $V_{\delta^{3\mu}}(x^*) \cap M_1 \neq \emptyset$. Let $x_n \in V_{\delta^{3\mu}}(x^*) \cap M_n$ be the unique minimizer of the functional $J_\alpha(x)$ in (2.16) on the set $G \cap M_n$ (Theorem 5.1). Let $x_{\alpha(\delta)} \in V_{\delta^{3\mu}/3}(x^*)$ be the unique regularized solution (Theorem 3.3). Assume that

$$x_n \neq x_{\alpha(\delta)}, \quad (5.3)$$

i.e. $x_{\alpha(\delta)} \notin M_n$, meaning that the regularized solution is not yet reached after n mesh refinements. Let $\eta \in (0, 1)$. Then one can choose the maximal grid size $h_{n+1} = h_{n+1}(N_1, N_2, \delta, B, K, \eta) \in (0, h_n]$ of the mesh refinement number $(n+1)$ so small that

$$\|x_{n+1} - x_{\alpha(\delta)}\| \leq \eta \|x_n - x_{\alpha(\delta)}\|, \quad (5.4)$$

where $x_{n+1} \in V_{\delta^{3\mu}}(x^*) \cap M_{n+1}$ is the unique minimizer of the functional (2.16) on the set $G \cap M_{n+1}$. Hence,

$$\|x_{n+1} - x_{\alpha(\delta)}\| \leq \eta^n \|x_1 - x_{\alpha(\delta)}\|. \quad (5.5)$$

Proof. In this proof we denote for brevity $\alpha(\delta) := \alpha$. Since $V_{\delta^{3\mu}}(x^*) \cap M_1 \neq \emptyset$, $M_1 \subseteq M_n$ and $V_{\delta^{3\mu}}(x^*) \subset V_1(x^*) \subset G$, then $(V_{\delta^{3\mu}}(x^*) \cap M_n) \subset (V_1(x^*) \cap M_{n+1}) \neq \emptyset$. Since by Theorem 3.2 the functional (2.16) is strongly convex on the set $V_{\delta^{3\mu}}(x^*)$ with the strong convexity constant $\alpha/4$, then Theorem 3.1 implies that

$$\frac{\alpha}{2} \|x_{n+1} - x_{\alpha(\delta)}\|^2 \leq (J'_\alpha(x_{n+1}) - J'_\alpha(x_{\alpha(\delta)}), x_{n+1} - x_{\alpha(\delta)}). \quad (5.6)$$

Since x_{n+1} is the minimizer on $G \cap M_{n+1}$ and x_α is the minimizer on the set G , then

$$(J'_\alpha(x_{n+1}), z) = 0, \quad \forall z \in M_{n+1}; \quad J'_\alpha(x_{\alpha(\delta)}) = 0. \quad (5.7)$$

Relations (5.7) justify the application of the Galerkin orthogonality principle [4, 6]. By (5.7)

$$(J'_\alpha(x_{n+1}) - J'_\alpha(x_{\alpha(\delta)}), x_{n+1} - P_{n+1}x_{\alpha(\delta)}) = 0. \quad (5.8)$$

Next, $x_{n+1} - x_{\alpha(\delta)} = (x_{n+1} - P_{n+1}x_{\alpha(\delta)}) + (P_{n+1}x_{\alpha(\delta)} - x_{\alpha(\delta)})$. Hence, (5.6) and (5.8) imply that

$$\frac{\alpha}{2} \|x_{n+1} - x_{\alpha(\delta)}\|^2 \leq (J'_\alpha(x_{n+1}) - J'_\alpha(x_{\alpha(\delta)}), P_{n+1}x_{\alpha(\delta)} - x_{\alpha(\delta)}). \quad (5.9)$$

It follows from (3.3) that conditions (5.2) and (5.3) imply that

$$\|J'_\alpha(x_{n+1}) - J'_\alpha(x_{\alpha(\delta)})\| \leq N_3 \|x_{n+1} - x_{\alpha(\delta)}\| \quad (5.10)$$

with a constant $N_3 = N_3(N_1, N_2) > 0$. Also, by (4.8)

$$\|x_{\alpha(\delta)} - P_{n+1}x_{\alpha(\delta)}\| \leq K \|x_{\alpha(\delta)}\| h_{n+1}. \quad (5.11)$$

Using the Cauchy-Schwarz inequality as well as (3.4), (5.10) and (5.11), we obtain from (5.9)

$$\|x_{n+1} - x_{\alpha(\delta)}\| \leq \frac{2KN_3}{\delta^{2\mu}} \|x_{\alpha(\delta)}\| h_{n+1}. \quad (5.12)$$

Since by one of conditions of Theorem 5.1 we have an *a priori* known upper estimate $\|x^*\| \leq B$, we now can estimate the norm $\|x_{\alpha(\delta)}\|$. Since by Theorem 3.3 $x_{\alpha(\delta)} \in V_{\delta^{3\mu}/3}(x^*)$, then

$$\|x_{\alpha(\delta)}\| \leq \|x_{\alpha(\delta)} - x^*\| + \|x^*\| \leq \frac{\delta^{3\mu}}{3} + B.$$

Hence, (5.12) becomes

$$\|x_{n+1} - x_{\alpha(\delta)}\| \leq \frac{2KN_3}{\delta^{2\mu}} \left(\frac{\delta^{3\mu}}{3} + B \right) h_{n+1}. \quad (5.13)$$

Let $\eta_n \in (0, 1)$ be an arbitrary number. Since $\|x_n - x_{\alpha(\delta)}\| \neq 0$, then we can choose $h_{n+1} = h_{n+1}(N_2, \delta, A, K) \in (0, h_n]$ so small that

$$\frac{2KN_3}{\delta^{2\mu}} \left(\frac{\delta^{3\mu}}{3} + B \right) h_{n+1} \leq \eta \|x_n - x_{\alpha(\delta)}\|. \quad (5.14)$$

Comparing (5.14) with (5.13), we obtain the target estimate (5.4). \square

Theorem 5.2 provides an estimate of the distance between points x_{n+1} obtained via adaptive mesh refinement and the regularized solution. We now estimate how far are these points from the exact solution x^* . Theorem 5.3 follows immediately from Theorem 2.2 and (5.5).

Theorem 5.3. *Let conditions of Theorem 5.2 hold. Let $\delta \in (0, \delta_0)$, where the number $\delta_0 \in (0, 1)$ is defined in Theorem 5.1. Then there exists a decreasing sequence of maximal grid step sizes $\{h_k\}_{k=1}^{n+1}$ such that*

$$\|x_{k+1} - x^*\| \leq \eta^k \|x_1 - x_{\alpha(\delta)}\| + \omega_F \left(2\delta^\mu \sqrt{A+1} \right), \quad k = 1, \dots, n, \quad (5.15)$$

where the number A is defined in (2.8) and the function ω_F is defined in (2.10), (2.11). In particular, let $\xi \in (0, 1)$ be an arbitrary number. Then there exists a sufficiently small number $\delta_1 = \delta_1(N_1, N_2, \mu, \xi) \in (0, \delta_0]$ and a decreasing sequence of maximal grid step sizes $\{h_k\}_{k=1}^{n+1}$ such that for all $\delta \in (0, \delta_1)$ and for $k \in [1, n]$

$$\|x_{k+1} - x^*\| \leq \eta^k \|x_1 - x_{\alpha(\delta)}\| + \begin{cases} \xi \|x_0 - x^*\|, & \text{if } x_0 \neq x^*, \\ \xi, & \text{if } x_0 = x^*. \end{cases} \quad (5.16)$$

Since h_{n+1} is the maximal grid step size in the entire domain Ω , it seems to be at the first glance that Theorems 5.2, 5.3 are about mesh refinements in the entire domain Ω rather than about local mesh refinements in subdomains, as it is the case in the adaptivity. Assuming that conditions of Theorem 5.2 hold, we now show that local mesh refinements are also covered by this theorem. Suppose that the domain Ω is split in two subdomains, $\Omega = \Omega_1 \cup \Omega_2, \Omega_1 \cap \Omega_2 = \emptyset$. Assume that the function x_0 is changing slowly in Ω_1 and has some ‘‘bumps’’ in Ω_2 . These bumps correspond to small inclusions. It is these inclusions rather than slowly changing functions, which are of the main applied interest in imaging. Indeed, those small abnormalities model, e.g. land mines, tumors, etc. Hence, it is reasonable to assume that x^* is also changing slowly in Ω_1 . Next, because of Theorem 2.2 and because all norms in H are equivalent, it is reasonable to assume that the regularized solution x_α is also changing slowly in Ω_1 . Thus, inequality (5.17) of Theorem 5.4 is a reasonable one. Furthermore, it is reasonable to assume that mesh refinements do not take place in Ω_1 , but only in Ω_2 .

Theorem 5.4 (relaxation for local mesh refinements). *Assume that conditions of Theorem 5.2 hold. Let $h^{(1)}$ be the maximal grid step size in Ω_1 . Then there exists a sufficiently small number $\delta_0 = \delta_0(N_1, N_2, \mu) \in (0, 1)$ and a decreasing sequence of maximal grid step sizes $\{\tilde{h}_k\}_{k=1}^{n+1}$ such that if the norm $\|\nabla x_{\alpha(\delta)}\|_{L^\infty(\Omega_1)}$ is so small that with the constant $N_3 = N_3(N_1, N_2) > 0$ from (5.10)*

$$\frac{2KN_3}{\delta^{2\mu}} \|\nabla x_{\alpha(\delta)}\|_{L^\infty(\Omega_1)} h^{(1)} \leq \frac{\eta}{2} \|x_k - x_{\alpha(\delta)}\|, k = 1, \dots, n, \quad (5.17)$$

then (5.15) and (5.16) hold with the replacement of $\{h_k\}_{k=1}^{n+1}$ with $\{\tilde{h}_k\}_{k=1}^{n+1}$.

Proof. By (5.9) and (5.10)

$$\begin{aligned} \|x_{k+1} - x_{\alpha(\delta)}\| &\leq \frac{2N_3}{\delta^{2\mu}} \|x_{\alpha(\delta)} - P_{k+1}x_{\alpha(\delta)}\| = \\ &\frac{2N_3}{\delta^{2\mu}} \left(\|x_{\alpha(\delta)} - P_{k+1}x_{\alpha(\delta)}\|_{L_2(\Omega_1)} + \|x_{\alpha(\delta)} - P_{k+1}x_{\alpha(\delta)}\|_{L_2(\Omega_2)} \right). \end{aligned} \quad (5.18)$$

By (4.7) and (5.17)

$$\frac{2N_3}{\delta^{2\mu}} \|x_{\alpha(\delta)} - P_{k+1}x_{\alpha(\delta)}\|_{L_2(\Omega_1)} \leq \frac{2KN_3}{\delta^{2\mu}} \|\nabla x_{\alpha(\delta)}\|_{L^\infty(\Omega_1)} h^{(1)} \leq \frac{\eta}{2} \|x_k - x_{\alpha(\delta)}\|. \quad (5.19)$$

Next, we obtain similarly with (5.14)

$$\frac{2N_3}{\delta^{2\mu}} \|x_{\alpha(\delta)} - P_{k+1}x_{\alpha(\delta)}\|_{L_2(\Omega_2)} \leq \frac{\eta}{2} \|x_k - x_{\alpha(\delta)}\|. \quad (5.20)$$

It follows from (5.18)-(5.20) that

$$\|x_{k+1} - x_{\alpha(\delta)}\| \leq \eta \|x_k - x_{\alpha(\delta)}\|, k = 1, \dots, n.$$

Hence, (5.5) holds. Finally, (5.16) follows from (5.5) and Theorem 2.2. \square

Remark 5.1. Theorems 5.3 and 5.4 claim that the accuracy of the solution improves with mesh refinements, i.e., the relaxation takes place. Comparison of (5.3) with (5.15) and (5.16) shows that the solution is adaptively refined until reaching the regularized solution $x_{\alpha(\delta)}$. It is important that by Theorem 2.2 the accuracy of $x_{\alpha(\delta)}$ is better than the accuracy of the first guess x_0 . Indeed, this ensures that it is worthy to work with the adaptivity in order to improve the accuracy of the regularized solution via mesh refinements.

6. Adaptivity for a Coefficient Inverse Problem. We now reformulate some of above theorems for the case of a specific CIP. To save space, we do not prove theorems of this section. Instead, we point to those results of Chapter 4 of [11] from which these theorems can be easily derived.

6.1. Coefficient Inverse Problem and Tikhonov functional. Let $\Omega \subset \mathbb{R}^3$ be a convex bounded domain with the boundary $\partial\Omega \in C^3$. Let the point $x_0 \notin \overline{\Omega}$. For $T > 0$ denote $Q_T = \Omega \times (0, T)$, $S_T = \partial\Omega \times (0, T)$. Let $d > 1$ be a certain number, $\omega \in (0, 1)$ be a sufficiently small number, and the function $c(x) \in C(\mathbb{R}^3)$ be such that

$$c(x) \in (1 - \omega, d + \omega) \text{ in } \Omega, c(x) = 1 \text{ outside of } \Omega. \quad (6.1)$$

Below we specify $c(x)$ more. Consider the solution $u(x, t)$ of the following Cauchy problem

$$c(x) u_{tt} = \Delta u, x \in \mathbb{R}^3, t \in (0, T), \quad (6.2)$$

$$u(x, 0) = 0, u_t(x, 0) = \delta(x - x_0). \quad (6.3)$$

Equation (6.2) governs propagation of acoustic waves, in which case $c(x) = 1/b^2(x)$, where $b(x)$ is the sound speed and $u(x, t)$ is the amplitude of the acoustic wave [22]. In addition, (6.2) governs propagation of the electromagnetic field in 2-d, in which case $c(x) = \varepsilon_r(x)$ is the spatially distributed dielectric constant and $u(x, t)$ is one of components of the electric field [44]. Although in the latter application equation (6.2) is valid only in 2-d, we have successfully used this equation to work with experimental data, which are obviously in 3-d, see [11, 15, 32] and section 8. This was explained in Test 4 of [18]. It was shown in this test that the component of the electric field, which was initially sent in a rather simple medium, dominates two other components. It was also shown that the propagation of the dominated component is well governed by equation (6.2).

Remark 6.1. An alternative to the point source in (6.3) is the incident plane wave in the case when it is initialized at the plane $\{x_3 = x_{3,0}\}$ such that $\{x_3 = x_{3,0}\} \cap \overline{\Omega} = \emptyset$. The formalism of derivations below is similar in this case. In our derivations below we focus on (6.3), because this is the most convenient case for derivations. However, in numerical studies we use the incident plane wave, because this case has shown a better performance than the point source.

Coefficient Inverse Problem (CIP). Let conditions (6.1)-(6.3) hold. Assume that the coefficient $c(x)$ is unknown inside the domain Ω . Determine this coefficient for $x \in \Omega$, assuming that the following function $g(x, t)$ is known

$$u|_{S_T} = g(x, t). \quad (6.4)$$

The function $g(x, t)$ can be interpreted as the result of measurements of the wave field $u(x, t)$ at the boundary of the domain of interest Ω . Since the function $c(x) = 1$ outside of Ω , then (6.2)-(6.4) imply

$$\begin{aligned} u_{tt} &= \Delta u, (x, t) \in (\mathbb{R}^3 \setminus \Omega) \times (0, T), \\ u(x, 0) &= u_t(x, 0) = 0, x \in \mathbb{R}^3 \setminus \Omega, u|_{S_T} = g(x, t). \end{aligned}$$

Solving this initial boundary value problem in the domain $\{(x, t) \in (\mathbb{R}^3 \setminus \Omega) \times (0, T)\}$, we uniquely obtain the Neumann boundary condition $p(x, t)$ for the function u ,

$$\partial_n u|_{S_T} = p(x, t). \quad (6.5)$$

CIPs are quite complex problems. Hence, to handle them, one naturally needs to impose some simplifying assumptions. In this particular CIP our theory of the adaptivity is not working unless we replace the δ -function in (6.3) by a smooth function, which approximates $\delta(x - x_0)$ in the distribution sense. Let $\varkappa \in (0, 1)$ be a sufficiently small number. We replace $\delta(x - x_0)$ in (6.3) with the function $\delta_\varkappa(x - x_0)$,

$$\delta_\varkappa(x - x_0) = \begin{cases} C_\varkappa \exp\left(\frac{1}{|x - x_0|^2 - \varkappa^2}\right), & |x - x_0| < \varkappa, \\ 0, & |x - x_0| > \varkappa, \end{cases} \quad \int_{\mathbb{R}^3} \delta_\varkappa(x - x_0) dx = 1. \quad (6.6)$$

We assume that \varkappa is so small that

$$\delta_\varkappa(x - x_0) = 0 \text{ in } \overline{\Omega}. \quad (6.7)$$

We now introduce state and adjoint problems. Let $\zeta \in (0, 1)$ be a sufficiently small number. Consider the function $z_\zeta \in C^\infty [0, T]$ such that

$$z_\zeta(t) = \begin{cases} 1, & t \in [0, T - 2\zeta], \\ 0, & t \in [T - \zeta, T], \\ \text{between 0 and 1} & \text{for } t \in [0, T - 2\zeta, T - \zeta]. \end{cases} \quad (6.8)$$

State Problem. Find the solution $v(x, t)$ of the following initial boundary value problem

$$\begin{aligned} c(x)v_{tt} - \Delta v &= 0 \text{ in } Q_T, \\ v(x, 0) = v_t(x, 0) &= 0, \\ \partial_n v|_{S_T} &= p(x, t). \end{aligned} \quad (6.9)$$

Adjoint Problem. Find the solution $\lambda(x, t)$ of the following initial boundary value problem with the reversed time

$$\begin{aligned} c(x)\lambda_{tt} - \Delta \lambda &= 0 \text{ in } Q_T, \\ \lambda(x, T) = \lambda_t(x, T) &= 0, \\ \partial_n \lambda|_{S_T} &= z_\zeta(t)(g - v)(x, t). \end{aligned} \quad (6.10)$$

Here functions $v \in H^1(Q_T)$ and $\lambda \in H^1(Q_T)$ are weak solutions of problems (6.9) and (6.10) respectively. In fact, we need a higher smoothness of these functions, which we specify below. In (6.9) and (6.10) functions g and p are the ones from (6.4) and (6.5) respectively. Hence, to solve the adjoint problem, one should solve the state problem first. The function $z_\zeta(t)$ is introduced to ensure the validity of compatibility conditions at $\{t = T\}$ in (6.10). The Tikhonov functional for the above CIP is

$$E_\alpha(c) = \frac{1}{2} \int_{S_T} (v|_{S_T} - g(x, t))^2 z_\zeta(t) d\sigma dt + \frac{1}{2} \alpha \int_{\Omega} (c - c_{glob})^2 dx, \quad (6.11)$$

where the function $c_{glob} \in C(\overline{\Omega})$ is the approximate solution obtained by our approximately globally convergent numerical method on the first stage of our two stage numerical procedure (section 1) and α is the small regularization parameter.

State and adjoint problems are concerned only with the domain Ω rather than with the entire space \mathbb{R}^3 . We define the space Z as

$$Z = \{f : f \in C(\overline{\Omega}) \cap H^1(\Omega), c_{x_i} \in L_\infty(\Omega), i = 1, 2, 3\}, \|f\|_Z = \|f\|_{C(\overline{\Omega})} + \sum_{i=1}^3 \|f_{x_i}\|_{L_\infty(\Omega)}.$$

Clearly $H \subset Z$ as a set. To apply the theory of above sections, we express in subsection 6.2 the function $c(x)$ via standard piecewise linear finite elements. Hence, we assume below that $c \in Y$, where

$$Y = \{c \in Z : c \in (1 - \omega, d + \omega)\}. \quad (6.12)$$

To find the Fréchet derivative of the functional $E_\alpha(c)$, we need to find Fréchet derivatives of functions solutions v, λ of problems (6.9), (6.10). This, in turn requires a higher smoothness of functions p, g [11, 14]. Theorem 6.1 can be easily derived from a combination of Theorems 4.7.1, 4.7.2 and 4.8 of [11] as well as from Theorems 3.1, 3.2 of [14].

Theorem 6.1. *Let $\Omega \subset \mathbb{R}^3$ be a convex bounded domain with the boundary $\partial\Omega \in C^2$ and such that there exists a function $a \in C^2(\overline{\Omega})$ such that $a|_{\partial\Omega} = 0, \partial_n a|_{\partial\Omega} = 1$. Assume that there exist functions $P(x, t), \Phi(x, t)$ such that*

$$\begin{aligned} P &\in H^6(Q_T), \Phi \in H^5(Q_T); \partial_n P|_{S_T} = p(x, t), \partial_n \Phi|_{S_T} = z_\zeta(t)g(x, t), \\ \partial_t^j P(x, 0) = \partial_t^j \Phi(x, 0) &= 0, j = 1, 2, 3, 4. \end{aligned}$$

Then for every function $c \in Y$ functions $v, \lambda \in H^2(Q_T)$, where v, λ are solutions of state and adjoint problems (6.9), (6.10). Also, for every $c \in Y$ there exists Fréchet derivative $E'_\alpha(c)$ of the Tikhonov functional $E_\alpha : Y \rightarrow \mathbb{R}$ in (6.11) and

$$E'_\alpha(c)(x) = \alpha(c - c_{glob})(x) - \int_0^T (u_t \lambda_t)(x, t) dt := \alpha(c - c_{glob})(x) + y(x). \quad (6.13)$$

Functions $E'_\alpha(c)(x), y(x) \in C(\overline{\Omega})$ and there exists a constant $D = D(\Omega, a, d, \omega, z_\zeta) > 0$ such that

$$\|y\|_{C(\overline{\Omega})} \leq \|c\|_{C(\overline{\Omega})}^2 \exp(DT) \left(\|P\|_{H^6(Q_T)}^2 + \|\Phi\|_{H^5(Q_T)}^2 \right). \quad (6.14)$$

The functional of the Fréchet derivative $E'_\alpha(c)$ acts on any function $b \in Z$ as

$$E'_\alpha(c)(b) = \int_\Omega E'_\alpha(c)(x) b(x) dx.$$

6.2. Relaxation property for the functional $E_\alpha(c)$. In this section we use Theorems 5.2, 5.4 to derive the relaxation property for the for the specific functional $E_\alpha(c)$ for our CIP. The first step is to define the operator F for our specific case. Set $G := Y \cap H$. We consider the set G as the subset of the space H with the same norm as the one in H . In particular, $\overline{G} = \{c(x) \in H : c(x) \in [1 - \omega, d + \omega] \text{ for } x \in \overline{\Omega}\}$. Let $H_2 := L_2(S_T)$. We define the operator F as

$$F : \overline{G} \rightarrow H_2, F(c)(x, t) = z_\zeta(t) [g(x, t) - v(x, t, c)], \quad (x, t) \in S_T, \quad (6.15)$$

where the function $v := v(x, t, c)$ is the weak solution (??) of the state problem (6.9), g is the function in (6.4) and $z_\zeta(t)$ is the function defined in (6.8). For any function $b \in H$ consider the weak solution $\tilde{u}(x, t, c, b) \in H^1(Q_T)$ of the following initial boundary value problem

$$\begin{aligned} c(x) \tilde{u}_{tt} &= \Delta \tilde{u} - b(x) v_{tt}, \quad (x, t) \in Q_T, \\ \tilde{u}(x, 0) &= \tilde{u}_t(x, 0) = 0, \quad \tilde{u}|_{S_T} = 0. \end{aligned}$$

Theorem 6.2 can be easily derived from a combination of Theorems 4.7.2 and 4.10 of [11].

Theorem 6.2. *Let $\Omega \subset \mathbb{R}^3$ be a convex bounded domain with the boundary $\partial\Omega \in C^2$. Suppose that there exist functions $a(x), P(x, t), \Phi(x, t)$ satisfying conditions of Theorem 6.1. Then the function $\tilde{u}(x, t, c, b) \in H^2(Q_T)$. Also, the operator F in (6.15) has the Fréchet derivative $F'(c)(b)$,*

$$F'(c)(b) = -z_\zeta(t) \tilde{u}(x, t, c, b)|_{S_T}, \quad \forall c \in G, \forall b \in H.$$

Let $B = B(\Omega, a, d, \omega, z_\zeta) > 0$ be the constant of Theorem 6.1. Then

$$\|F'(c)\|_{\mathcal{L}} \leq \exp(CT) \left(\|P\|_{H^6(Q_T)} + \|\Phi\|_{H^5(Q_T)} \right), \quad \forall c \in G.$$

In addition, the operator $F'(c)$ is Lipschitz continuous,

$$\|F'(c_1) - F'(c_2)\|_{\mathcal{L}} \leq \exp(CT) \left(\|P\|_{H^6(Q_T)} + \|\Phi\|_{H^5(Q_T)} \right) \|c_1 - c_2\|, \quad \forall c_1, c_2 \in G.$$

Following (2.2), we introduce the error of the level δ in the data $g(x, t)$ in (6.4). So, we assume that

$$g(x, t) = g^*(x, t) + g_\delta(x, t); \quad g^*, g_\delta \in L_2(S_T), \|g_\delta\|_{L_2(S_T)} \leq \delta. \quad (6.16)$$

where $g^*(x, t)$ is the exact data and the function $g_\delta(x, t)$ represents the error in these data. To make sure that the operator F is one-to-one, we need to refer to a uniqueness theorem for our CIP. However,

uniqueness results for multidimensional CIPs with single measurement data are currently known only under the assumption that at least one of initial conditions does not equal zero in the entire domain $\overline{\Omega}$, which is not our case. All these theorems were proven by the method, which was originated in 1981 in three papers [19, 20, 28]; also see, e.g. [21, 29, 30, 31, 34, 35] as well as sections 1.10, 1.11 of the book [11] and references cited there for some follow up publications of those authors about this method. This method is based on Carleman estimates. Although many other researchers have published about this method, we do not cite those works here, because the topic of uniqueness is not a focus of the current paper. We refer to surveys [35, 48] for more references. Lifting the above assumption is a long standing and well known open question, see [34] for a recent partial answer to this question. Nevertheless, because of applications, it makes sense to develop numerical methods for the above CIP, regardless on the absence of proper uniqueness theorems. Therefore, we introduce Assumption 6.1.

Assumption 6.1. *The operator $F(c)$ defined in (6.15) is one-to-one.*

Theorem 6.3 follows from Theorems 3.3, 6.1 and 6.2. Note that if a function $c \in H$ is such that $c \in [1, d]$, then by (6.12) $c \in G$.

Theorem 6.3. *Let $\Omega \subset \mathbb{R}^3$ be a convex bounded domain with the boundary $\partial\Omega \in C^3$. Suppose that there exist functions $a(x), P(x, t), \Phi(x, t)$ satisfying conditions of Theorem 6.1. Let Assumption 6.1 and condition (6.16) hold. Let the function $v = v(x, t, c) \in H^2(Q_T)$ in (6.11) be the solution of the state problem (6.9) for the function $c \in G$. Assume that there exists the exact solution $c^* \in G, c^*(x) \in [1, d]$ of the equation $F(c^*) = 0$ for the case when in (6.16) the function g is replaced with the function g^* . Let in (6.16)*

$$\alpha = \alpha(\delta) = \delta^{2\mu}, \mu = \text{const.} \in (0, 1/4).$$

Also, let in (6.11) the function $c_{glob} \in G$ and

$$\|c_{glob} - c^*\| < \frac{\delta^{3\mu}}{3}.$$

Then there exists a sufficiently small number $\delta_0 = \delta_0(\Omega, d, \omega, z_\zeta, a, \|P\|_{H^6(Q_T)}, \|\Phi\|_{H^5(Q_T)}, \mu) \in (0, 1)$ such that $V_{\delta^{3\mu}}(c^*) \subset G, \forall \delta \in (0, \delta_0)$ and the functional $E_\alpha(c)$ is strongly convex in $V_{\delta^{3\mu}}(c^*)$ with the strong convexity constant $\alpha/4$. In other words,

$$\|c_1 - c_2\|^2 \leq \frac{2}{\delta^{2\mu}} (E'_\alpha(c_1) - E'_\alpha(c_2), c_1 - c_2), \forall c_1, c_2 \in V_{\delta^{3\mu}}(c^*), \quad (6.17)$$

where (\cdot, \cdot) is the scalar product in $L_2(\Omega)$ and the Fréchet derivative E'_α is calculated via (6.13). Furthermore, there exists the unique regularized solution $c_{\alpha(\delta)}$, and $c_{\alpha(\delta)} \in V_{\delta^{3\mu/3}}(x^*)$. In addition, the gradient method of the minimization of the functional $E_\alpha(c)$, which starts at c_{glob} , converges to $c_{\alpha(\delta)}$. Furthermore, let $\xi \in (0, 1)$ be an arbitrary number. Then there exists a number $\delta_1 = \delta_1(\Omega, d, \omega, z_\zeta, a, \|P\|_{H^6(Q_T)}, \|\Phi\|_{H^5(Q_T)}, \mu, \xi) \in (0, \delta_0)$ such that for all $\delta \in (0, \delta_1)$

$$\|c_{\alpha(\delta)} - c^*\| \leq \begin{cases} \xi \|c_{glob} - c^*\|, & \text{if } c_{glob} \neq c^*, \\ \xi, & \text{if } c_{glob} = c^*. \end{cases}$$

In other words, the regularized solution $c_{\alpha(\delta)}$ is more accurate than the solution obtained on the first stage of our two-stage numerical procedure. Furthermore, since $E'_{\alpha(\delta)}(c_{\alpha(\delta)}) = 0$, then (6.17) implies that

$$\|c - c_{\alpha(\delta)}\| \leq \frac{2}{\delta^{2\mu}} \|E'_{\alpha(\delta)}(c)\|_{L_2(\Omega)}, \forall c \in V_{\delta^{3\mu}}(c^*).$$

Theorem 6.4 follows from Theorems 5.1 and 6.3 as well as from Theorem 4.11.3 of [11].

Theorem 6.4. *Let conditions of Theorem 6.3 hold. Let $\|c^*\| \leq B$, where the constant B is given. Let $M_n \subset H$ be the subspace obtained after n mesh refinements as described in section 4. Let h_n be the maximal*

grid step size of the subspace M_n . Let $D = D(\Omega, a, d, \omega, z_\zeta) > 0$ be the constant of Theorem 6.1 and K be the constant in (4.8). There exists a constant $\overline{N}_2 = \overline{N}_2(D, T, \|P\|_{H^6(Q_T)}, \|\Phi\|_{H^5(Q_T)})$ such that if

$$h_n \leq \frac{\delta^{4\mu}}{5B\overline{N}_2K},$$

then there exists the unique minimizer c_n of the functional (6.11) on the set $G \cap M_n$. Furthermore, $c_n \in V_{\delta^{3\mu}}(x^*) \cap M_n$ and the following a posteriori error estimate holds

$$\|c_n - c_{\alpha(\delta)}\| \leq \frac{2}{\delta^{2\mu}} \left\| E'_{\alpha(\delta)}(c_n) \right\|_{L_2(\Omega)}. \quad (6.18)$$

The estimate (6.18) is a *posteriori* because it is obtained after the function c_n is calculated. Theorem 6.5 follows from Theorems 5.2, 5.3, 6.4, also see Theorem 4.11.4 in [11].

Theorem 6.5 (relaxation). *Assume that conditions of Theorem 6.4 hold. Let $c_n \in V_{\delta^{3\mu}}(x^*) \cap M_n$ be the unique minimizer of the Tikhonov functional (6.11) on the set $G \cap M_n$ (Theorem 6.4). Assume that the regularized solution $c_{\alpha(\delta)} \neq c_n$, i.e. $c_{\alpha(\delta)} \notin M_n$. Let $\eta \in (0, 1)$ be an arbitrary number. Then one can choose the maximal grid size $h_{n+1} = h_{n+1}(B, \overline{N}_2, K, \delta, z_\zeta, \mu, \eta) \in (0, h_n]$ of the mesh refinement number $(n+1)$ so small that*

$$\|c_{n+1} - c_{\alpha(\delta)}\| \leq \eta \|c_n - c_{\alpha(\delta)}\|, \quad (6.19)$$

where the number \overline{N}_2 was defined in Theorem 6.4. Let $\xi \in (0, 1)$ be an arbitrary number. Then there exists a sufficiently small number $\delta_0 = \delta_0(A, \overline{N}_2, K, \delta, z_\zeta, \xi, \mu, \eta) \in (0, 1)$ and a decreasing sequence of maximal grid step sizes $\{h_k\}_{k=1}^{n+1}$, $h_k = h_k(B, \overline{N}_2, K, \delta, z_\zeta, \xi, \mu, \eta)$ such that if $\delta \in (0, \delta_0)$, then

$$\|c_{k+1} - c^*\| \leq \eta^k \|c_1 - c_{\alpha(\delta)}\| + \begin{cases} \xi \|c_{glob} - c^*\|, & \text{if } c_{glob} \neq c^*, \\ \xi, & \text{if } c_{glob} = c^*, \end{cases} \quad , k = 1, \dots, n. \quad (6.20)$$

Theorem 6.6 follows from Theorems 5.4 and 6.5.

Theorem 6.6. (relaxation for local mesh refinements). *Assume that conditions of Theorem 6.5 hold. Let $\Omega = \Omega_1 \cup \Omega_2$. Suppose that mesh refinements are performed only in the subdomain Ω_2 . Let $h^{(1)}$ be the maximal grid step size in Ω_1 . Then there exists a sufficiently small number $\delta_0 = \delta_0(B, \overline{N}_2, K, z_\zeta, \mu, \eta) \in (0, 1)$ and a decreasing sequence of maximal grid step sizes $\{\tilde{h}_k\}_{k=1}^{n+1}$, $\tilde{h}_k = \tilde{h}_k(B, \overline{N}_3, K, z_\zeta, \mu, \eta)$ of meshes in Ω_2 such that if $\|\nabla c_{\alpha(\delta)}\|_{L_\infty(\Omega_1)}$ is so small that if*

$$\frac{2K\overline{N}_3}{\delta^{2\mu}} \|\nabla c_{\alpha(\delta)}\|_{L_\infty(\Omega_1)} h^{(1)} \leq \frac{\eta}{2} \|c_k - c_{\alpha(\delta)}\|, \quad k = 1, \dots, n \text{ and } \delta \in (0, \delta_0),$$

then (6.20) holds with the replacement of $\{h_k\}_{k=1}^{n+1}$ with $\{\tilde{h}_k\}_{k=1}^{n+1}$.

Here the number $\overline{N}_3 = \overline{N}_3(D, T, \|P\|_{H^6(Q_T)}, \|\Phi\|_{H^5(Q_T)}) > 0$.

7. Mesh Refinement Recommendations and the Adaptive Algorithm.

7.1. Mesh Refinement Recommendations. Recommendations for mesh refinements are based on the theory of section 6. We now present some partly rigorous and partly heuristic considerations which lead to these recommendations. The latter means that both mesh refinement recommendations listed below should be verified numerically. We come back to the arguments presented in the paragraph above Theorem 5.4. To simplify the presentation, assume, for example that

$$\nabla c_{\alpha(\delta)}(x) = \nabla c^*(x) = 0 \text{ for } x \in \Omega_1. \quad (7.1)$$

A more general case when functions $c_{\alpha(\delta)}(x), c^*(x)$ change slowly in Ω_1 can be considered similarly. Using (4.7) and (7.1), we obtain that $(c_{\alpha(\delta)} - P_k c_{\alpha(\delta)})(x) = 0$ for $x \in \Omega_1, \forall k \geq 1$. Hence, by (4.7)

$$\|c_{\alpha(\delta)} - P_{n+1} c_{\alpha(\delta)}\|_{L_2(\Omega)} = \|c_{\alpha(\delta)} - P_{n+1} c_{\alpha(\delta)}\|_{L_2(\Omega_2)} \leq K \|\nabla c_{\alpha(\delta)}\|_{L_\infty(\Omega_2)} \tilde{h}_{n+1},$$

where \tilde{h}_{n+1} is the maximal grid step size in Ω_2 after $n+1$ mesh refinements. Hence, using the second equality (5.7) and (5.9), we obtain

$$\|c_{n+1} - c_{\alpha(\delta)}\| \leq \frac{2K}{\delta^{2\mu}} \|E'_{\alpha(\delta)}(c_{n+1})\| \|\nabla c_{\alpha(\delta)}\|_{L_\infty(\Omega_2)} \tilde{h}_{n+1}. \quad (7.2)$$

Given a function $f \in C(\bar{\Omega})$, the main impact in the norm $\|f\|_{L_2(\Omega)}$ is provided by neighborhoods of those points $x \in \bar{\Omega}$ where the function $|f(x)|$ achieves its maximal value. Hence, (7.2) indicates that we should decrease the maximal grid step size \tilde{h}_{n+1} (i.e. refine mesh) in neighborhoods of those points $x \in \Omega_2$ where the function $|E'_{\alpha(\delta)}(c_{n+1})(x)|$ achieves its maximal values, where the function $E'_{\alpha(\delta)}(c_{n+1})(x) \in C(\bar{\Omega})$ is given by formula (6.13). Although after n mesh refinements we know only the function $c_n \in M_n$ rather than the function $c_{n+1} \in M_{n+1}$, still, since functions c_n and c_{n+1} are sufficiently close to each other, we should likely refine mesh in neighborhoods of those points $x \in \Omega_2$ where the function $|E'_\alpha(c_n)(x)|$ achieves its maximal values. These considerations lead to two mesh refinement recommendations below.

The First Mesh Refinement Recommendation. Let $\beta_1 \in (0, 1)$ be the tolerance number. Refine the mesh in such subdomains of Ω_2 where

$$|E'_\alpha(c_n)(x)| \geq \beta_1 \max_{\bar{\Omega}_2} |E'_\alpha(c_n)(x)|. \quad (7.3)$$

To figure out the second mesh refinement recommendation, we note that by (6.13) and (6.14)

$$\left| E'_{\alpha(\delta)}(c_n)(x) \right| \leq \alpha \left(\|c_n\|_{C(\bar{\Omega})} + \|c_{glob}\|_{C(\bar{\Omega})} \right) + \|c_n\|_{C(\bar{\Omega})}^2 \exp(DT) \left(\|P\|_{H^6(Q_T)}^2 + \|\Phi\|_{H^5(Q_T)}^2 \right).$$

Since α is small, then the second term in the right hand side of this estimate dominates. Next, since we have decided to refine the mesh in neighborhoods of those points, which deliver maximal values for the function $|E'_{\alpha(\delta)}(c_n)(x)|$, then we obtain the following mesh refinement recommendation.

Second Mesh Refinement Recommendation. Let $\beta_2 \in (0, 1)$ be the tolerance number. Refine the mesh in such subdomains of Ω_2 where

$$c_n(x) \geq \beta_2 \max_{\bar{\Omega}_2} c_n(x), \quad (7.4)$$

In fact, these two mesh refinement recommendations do not guarantee of course that the minimizer obtained on the corresponding finer mesh would be indeed more accurate than the one obtained on the coarser mesh. This is because right hand sides of formulas (7.3) and (7.4) are indicators only. Thus, numerical verifications are necessary. As to tolerance numbers β_1 and β_2 , they should be chosen numerically. Indeed, if we would choose $\beta_1, \beta_2 \approx 1$, then we would refine the mesh in too narrow regions. On the other hand, if we would choose $\beta_1, \beta_2 \approx 0$, then we would refine the mesh in almost the entire subdomain Ω_2 , which is inefficient.

7.2. The adaptive algorithm. Since this algorithm was described in detail in a number of publications, see, e.g. [11, 14], we outline it only briefly here. Recall that the adaptivity is used on the second stage of our two-stage numerical procedure (section 1). On the first stage the approximately globally convergent algorithm is applied. It was proven, within the framework of the so-called Second Approximate Mathematical Model, that this algorithm delivers a good approximation for the exact solution $c^*(x)$ of the above CIP, see Theorem 2.9.4 in [11] as well as Theorem 5.1 in [17]. We start the adaptivity on the same mesh on which the algorithm of the first stage has worked. In our experience, this mesh does not provide an improvement

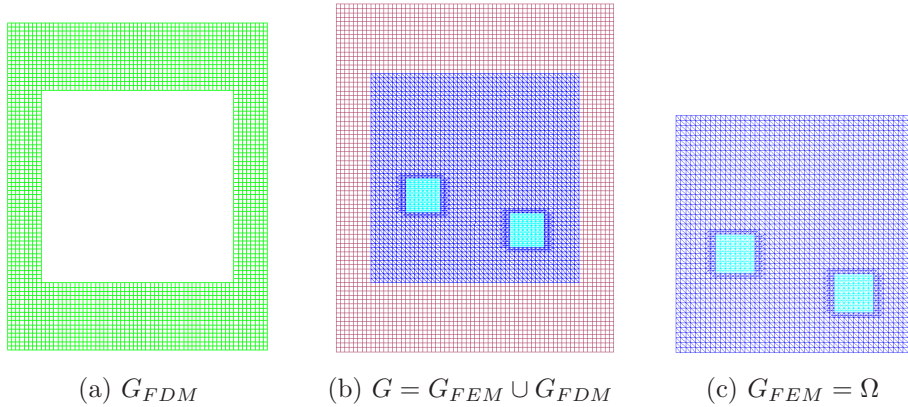


Fig. 8.1: The hybrid mesh (b) is a combinations of a structured mesh (a), where FDM is applied, and a mesh (c), where we use FEM, with a thin overlapping of structured elements. The solution of the inverse problem is computed in the square Ω and $c(x) = 1$ for $x \in G \setminus \Omega$.

of the image. On each mesh we find an approximate solution of the equation $E'_\alpha(c) = 0$. Hence, by (6.13) we find an approximate solution of the following equation on each mesh

$$\alpha(c - c_{glob})(x) - \int_0^T (u_t \lambda_t)(x, t) dt = 0.$$

For each newly refined mesh we first linearly interpolate the function $c_{glob}(x)$ on it. Since this function was initially computed as a linear combination of finite elements forming the initial mesh and since all our finite elements are piecewise linear functions, then subsequent linear interpolations on finer meshes do not change the function $c_{glob}(x)$. On each mesh we iteratively update approximations c_α^n of the function $c_{\alpha(\delta)}$. To do this, we use the quasi-Newton method with the classic BFGS update formula with the limited storage [42]. Denote

$$\varphi^n(x) = \alpha(c_\alpha^n - c_{glob})(x) - \int_0^T (v_{ht} \lambda_{ht})(x, t, c_\alpha^n) dt,$$

where functions $v_h(x, t, c_\alpha^n)$, $\lambda_h(x, t, c_\alpha^n)$ are FEM solutions of state and adjoint problems (6.9), (6.10) with $c := c_\alpha^n$. We stop computing c_α^n if either $\|\varphi^n\|_{L_2(\Omega)} \leq 10^{-5}$ or norms $\|\varphi^n\|_{L_2(\Omega)}$ are stabilized. Of course, only discrete norms are considered here.

For a given mesh obtained after n mesh refinements, let c_n be the last computed function on which we have stopped. Next, we compute the function $|E'_\alpha(c_n)(x)|$ using (6.13), where $v := v_h(x, t, c_n)$, $\lambda := \lambda_h(x, t, c_n)$. If we use both above mesh refinement recommendations, then we refine the mesh in neighborhoods of all grid points satisfying (7.3) and (7.4). In some studies, however, we use only the first recommendation. In this case we refine the mesh in neighborhoods of all grid points satisfying only (7.3).

8. Numerical Studies. We present here three numerical examples of the performance of our two-stage numerical procedure: one for computationally simulated and two for experimental data. More numerical tests of the adaptivity technique can be found in [1, 6, 7, 8, 9, 10, 11, 13, 14, 15, 16]. In Test 1 we have used only the First Mesh Refinement Recommendation, and in Tests 2,3 we have used both recommendations. Since the numerical method of the first stage of our procedure is not a focus of this paper, and since it was described earlier in, e.g. [11, 13, 14, 15, 32, 37, 38], we do not describe it here.

8.1. Computationally simulated data. Test 1. We conducted computational simulations in two dimensions. Since it is impossible to computationally solve equation (6.2) in the entire space \mathbb{R}^2 , we have conducted data simulations in the rectangle $G = [-4, 4] \times [-5, 5]$. To simulate the boundary data $g(x, t)$, we have solved the forward problem by the hybrid FEM/FDM method [5] using the software package WavES [47]. To do this, we split the domain G in two subdomains $G = G_{FEM} \cup G_{FDM}$, see Figure 8.1. Here $G_{FEM} := \Omega = [-3, 3] \times [-3, 3]$ and $G_{FDM} = G \setminus G_{FEM}$. The coefficient $c(x)$ is unknown in the domain $\Omega \subset G$ and is defined as

$$c(x) = \begin{cases} 1 & \text{in } G_{FDM}, \\ 1 + b(x) & \text{in } G_{FEM}, \\ 4 & \text{in small squares of Figure 8.1,} \end{cases} \quad (8.1)$$

where the function $b(x) \in \Omega_{FEM}$ is defined as

$$b(x) = \begin{cases} 0 & \text{for } (x_1, x_2) \in \Omega_{FEM} : -2.875 < x_1 < 0, -2.875 < x_2 < 0, \\ 0.5 \sin^2\left(\frac{\pi x_1}{2.875}\right) \sin^2\left(\frac{\pi x_2}{2.875}\right) & \text{otherwise.} \end{cases}$$

The spatial mesh consists of triangles in G_{FEM} and of squares in G_{FDM} with the grid step size $\bar{h} = 0.125$ both in overlapping regions and in G_{FDM} . There is no reason to refine mesh in G_{FDM} since $c(x) = 1$ in G_{FDM} . Let ∂G_1 and ∂G_2 be, respectively, top and bottom sides of the rectangle G and ∂G_3 be the union of vertical sides of G . We use first order absorbing boundary conditions on $\partial G_1 \cup \partial G_2$ [24] and zero Neumann boundary condition on ∂G_3 .

Let \bar{s} be the upper value of the Laplace transform of the solution of our forward problem. We use this transform on the first stage of our two-stage numerical procedure. It was found that for the above domain Ω the optimal value is $\bar{s} = 7.45$. Consider the function $f(t)$,

$$f(t) = \begin{cases} 0.1 [\sin(\bar{s}t - \pi/2) + 1], & t \in [0, t_1], t_1 = 2\pi/\bar{s}, \\ 0, & t \in (t_1, T], T = 17.8t_1. \end{cases}$$

The forward problem for data simulations is

$$\begin{aligned} c(x) u_{tt} - \Delta u &= 0, & \text{in } G \times (0, T), \\ u(x, 0) &= 0, \quad u_t(x, 0) = 0, & \text{in } G, \\ \partial_n u|_{\partial G_1} &= f(t), & \text{on } \partial G_1 \times (0, t_1], \\ \partial_n u|_{\partial G_1} &= -\partial_t u, & \text{on } \partial G_1 \times (t_1, T), \\ \partial_n u|_{\partial G_2} &= -\partial_t u, & \text{on } \partial G_2 \times (0, T), \\ \partial_n u|_{\partial G_3} &= 0, & \text{on } \partial G_3 \times (0, T). \end{aligned} \quad (8.2)$$

The solution of this problem gives us the function $g(x, t) = u|_{S_T}$. Next, the coefficient $c(x)$ is ‘‘forgotten’’ and we apply the two-stage numerical procedure to reconstruct it from the function $g(x, t)$. To have noisy data, we have added the random noise to the function $g(x, t)$ as

$$g_{i,j} = g(x^i, t^j) [1 + 0.02\alpha_j (g_{\max} - g_{\min})]. \quad (8.3)$$

Here $x^i \in \partial\Omega$ and $t^j \in [0, T]$ are mesh points on $\partial\Omega$ and $[0, T]$ respectively, g_{\min} and g_{\max} are minimal and maximal values of the function g and $\alpha_j \in [-1, 1]$ is the random variable. The ‘‘inverse crime’’ was not committed here since we have introduced the noise in the data and because the grids in both stages of our two-stage numerical procedure were different from the one which was used to solve the problem (8.2).

1. *The approximately globally convergent stage.* Since we focus on the adaptivity in this paper, we do not describe this algorithm here and refer to section 2.6.1 of [11] instead. Figure 8.2 displays the result of this stage.

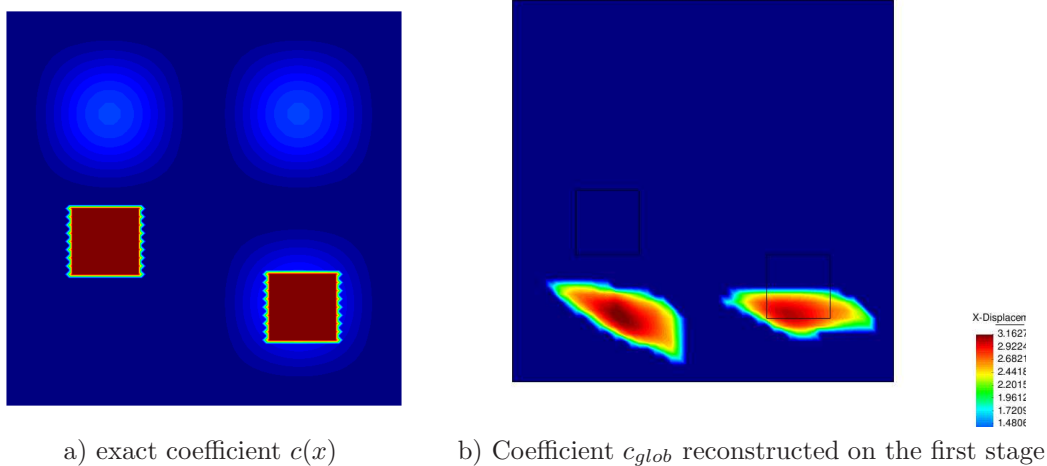


Fig. 8.2: a) Spatial distribution of the exact coefficient $c(x)$. b) Result of the performance of the approximately globally convergent algorithm (first stage). The spatial distribution of the computed coefficient c_{glob} displayed. Here $\max c_{glob}(x) = 3.2$, whereas $\max c(x) = 4$. Hence, we have 20% error in imaging of the maximal value of the function $c(x)$. The slowly changing part of the function $c(x)$, i.e. the second row in the above definition of the function $b(x)$, is not imaged. Comparison with Figure a) shows that while the location of the right inclusion is imaged correctly, the left one still needs to be moved upwards. This is done on the second stage of our two-stage numerical procedure, i.e. on the adaptivity stage. On this stage we take the function $c_{glob}(x)$ as the starting point for the minimization of the Tikhonov functional (6.11). The second stage refines the image of the first.

2. *The adaptivity stage.* Since we have observed that $u(x, T) \approx 0$, we have not used the function $z_\zeta(t)$ in our computations. In this test we take the noise level 2% in (8.3) and the regularization parameter $\alpha = 0.02$ in (6.11). We now comment on the stopping criterion for mesh refinements, which we use in numerical studies of the adaptivity technique in this paper. Let c_n is the coefficient $c(x)$ calculated after n mesh refinements. In Theorems 5.2-5.4, 6.5, 6.6 the relaxation parameter η is independent on the mesh refinement number n . In practice, however, one should expect such dependence $\eta := \eta_n$. In this case the parameter η of those theorems is $\eta = \max(\eta_n)$. Then because of the relaxation property of Theorems 6.5, 6.6 as well as because of Remark 5.1, it is anticipated that numbers η_n decrease with the grow of n until the regularized solution $c_{\alpha(\delta)}$ is approximately reached. However, nothing can be guaranteed about numbers η_n as soon as the regularized solution is reached. Hence, in our computations of the adaptivity method we stopped mesh refinement process at such $n := n_0$ that $\eta_{n_0} > \eta_{n_0-1}$. If $\eta_{n_0} \approx \eta_{n_0-1}$, then we took the final solution $c_{final} := c_{n_0}$.

Figure 8.3-e), f) represents the images obtained after 4 and 5 mesh refinements, respectively, as well as adaptive locally refined meshes are presented on 8.3-a)-d). Comparing with Figure 8.1-c), one can observe that locations of both inclusions are imaged accurately. Recall that in each inclusion of Figure 8.1-c) $c(x) = 4$, see definition for $c(x)$ in (8.1) shown also on Figure 8.2-a). Therefore, maximal values of the function $c(x)$ on Figures 8.3-e), f) are also accurately imaged: the error does not exceed 3.5%.

Figure 8.4 displays the graph of the dependence of the norm $\|c_n - c_\alpha\|_{L_2(\Omega)}$ from the mesh refinement number n . By (6.19) and (6.20) these norms should decay. Since we do not exactly know what the regularized solution c_α is, we have taken $c_\alpha := c_4$ on Figure 8.4-a). On Figure 8.4-b) we have superimposed those graphs for $c_\alpha := c_4$ and $c_\alpha := c_5$. One can observe that norms $\|c_n - c_\alpha\|$ decay in the case when c_α is taken on the 4-th refined mesh. At the same time we also observe, that the relaxation property (6.20) is not fulfilled when we take c_α on the 5-th refined mesh since $\eta_3 > \eta_2$, see 8.4-b). Thus, we take the final reconstruction $c_\alpha := c_4$, the function obtained after four (4) mesh refinements.

Remark 8.1. It is well known that imaging of locations of small inclusions and maximal values of the

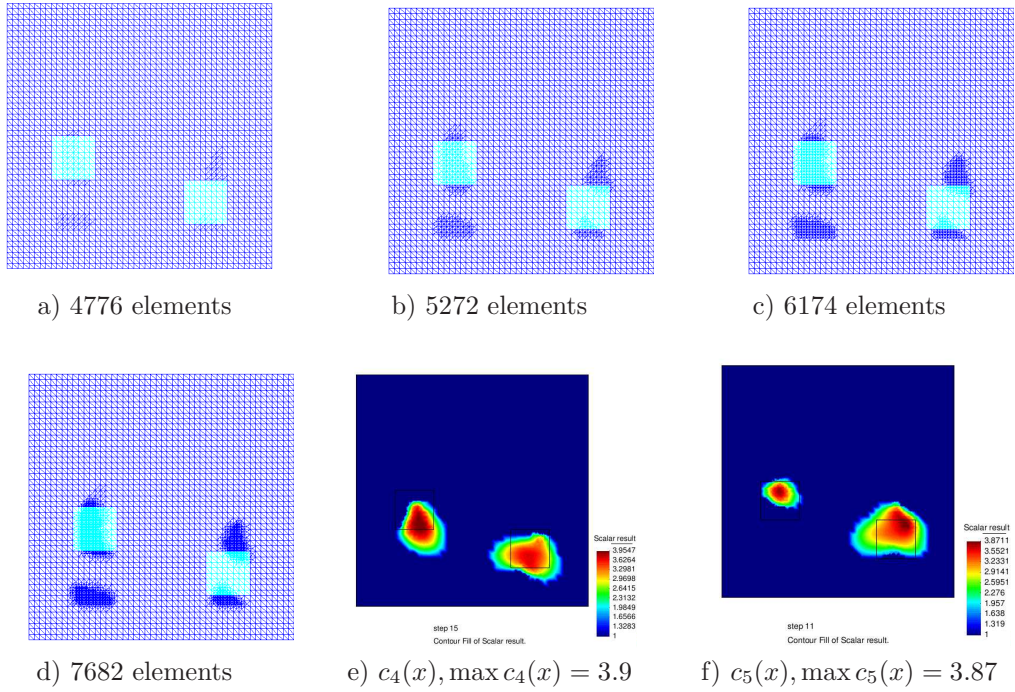


Fig. 8.3: Adaptively refined meshes (a)–(d) and finally reconstructed images (e) and (f) on 4-th and 5-th adaptively refined meshes, respectively. On e) $\max c_4 = 3.9$ and on f) $\max c_5 = 3.87$. Reconstructed function on e) is obtained on the mesh presented on d). The mesh for the function on f) is not shown. Locations of both squares of Figure 8.3-a) as well as maximal values of the computed function $c_{glob}(x)$ in them are imaged accurately.

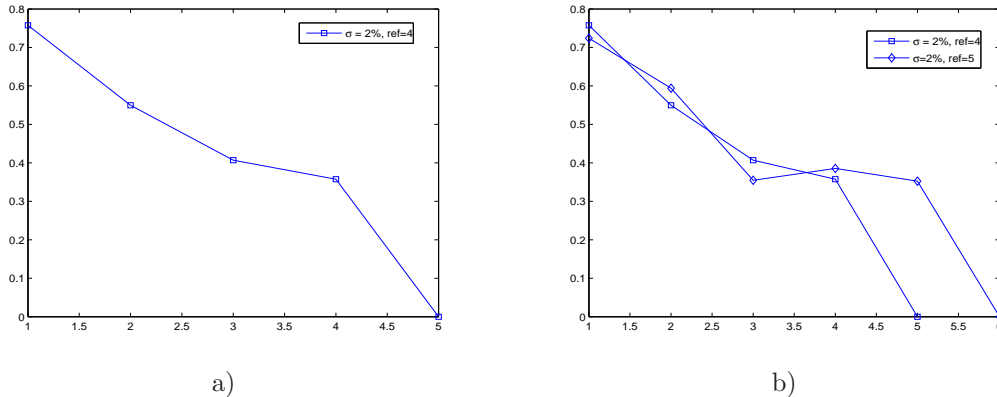


Fig. 8.4: a) Computed relaxation property $\|c_{n+1} - c_\alpha\|_{L_2} \leq \eta_n \|c_n - c_\alpha\|_{L_2}$ for the noise level 2% in (8.3) and the regularization parameter $\alpha = 0.02$ in (6.11). Here, $0 < \eta_n < 1$ is the small relaxation parameter obtained after n mesh refinements. Here, we take c_α on the 4-th refined mesh shown on the Figure 8.3-d). b) Comparison of the relaxation property $\|c_{n+1} - c_\alpha\|_{L_2} \leq \eta_n \|c_n - c_\alpha\|_{L_2}$ when we take different functions c_α : on the 4-th or on the 5-th refined mesh.

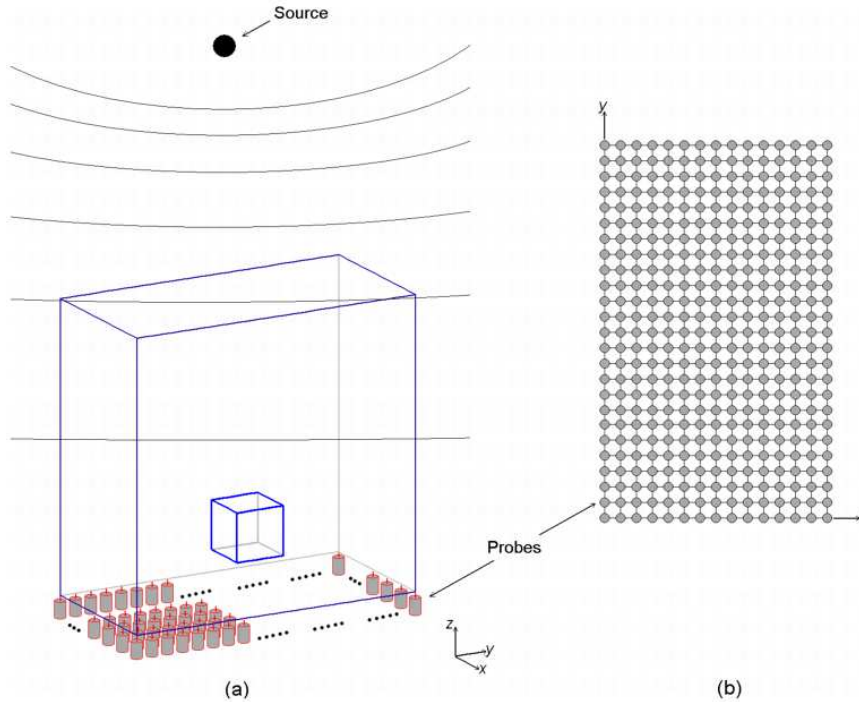


Fig. 8.5: Schematic diagram of data collection. Original source: M. V. Klibanov, M. A. Fiddy, L. Beilina, N. Pantong and J. Schenk, *Picosecond scale experimental verification of a globally convergent numerical method for a coefficient inverse problem*, *Inverse Problems*, 26, 045003, doi:10.1088/0266-5611/26/4/045003, 2010. ©IOP Publishing. Reprinted with permission.

function $c(x)$ in them is of the primary interest in applications and it is more interesting than imaging of slowly changing parts. Indeed, small inclusions can be explosives [37, 38], tumors, etc..

Remark 8.2. The above stopping criterion for mesh refinements shows that relaxation Theorems 6.5, 6.6 are quite useful for computations.

8.2. Experimental data. Experimental studies were described in detail in [15, 32] as well as in Chapter 5 of [11]. Hence, we omit many details here. We point out that the main difficulty was a *huge misfit* between computationally simulated and experimental data. The latter was the case even for the free space data: the analytic solution predicted by Maxwell equations was radically different from the experimentally measured curves. This can be explained by unknown nonlinear processes in both transmitters and detectors. The same was observed for the backscattering data collected in the field, see [38] and section 6.9 of [11]. To handle this misfit, a new data pre-processing procedure was applied. This procedure has immersed experimental data in computationally simulated ones, see Figures 4 in [38] and Figures 5.3 in [11]. Naturally, this procedure has introduced a significant modeling noise in already noisy data. Nevertheless, computational results were very accurate ones, which speaks well for the robustness of our reconstruction method. The first stage of our two-stage numerical procedure was working with *blind* data (unlike the second stage). Therefore, results of at least the first stage were unbiased.

The data collection scheme is displayed on Figure 8.5. A single source of electric wave field emits pulse for only one component of the electric field, two other components were not emitted. The prism is our computational domain Ω . The outcome time resolved signal was measured at many detectors located on the bottom side of the prism. The same component of the electric field was measured as the one emitted. Since

Case number	Computed n	Directly measured n	Computational error
1 (Cube 1)	1.97	2.07	5%
2 (Cube 1)	2	2.07	3.4%
3 (Cube 1)	2.16	2.07	4.3%
4 (Cube 1)	2.19	2.07	5.8%
5 (Cube 2)	1.73	1.71	1.2%
6 (Cube 2)	1.79	1.71	4.7%

Table 8.1: Blindly computed and directly measured refractive indices n by the first stage of our two-stage numerical procedure. The error in direct measurements was 11% for cases 1-4 (Cube 1) and 3.5% for cases 5,6 (Cube 2).

we have not measured that signal at the rest $\partial_1\Omega$ of $\partial\Omega$, we have prescribed to $\partial_1\Omega$ the same boundary conditions as ones for the uniform medium with the dielectric constant $\varepsilon_r \equiv 1$. The prism Ω is filled with a dielectric material with the dielectric constant $\varepsilon_r \approx 1$, i.e. almost the same as in the air. We point out, however, that when using the first stage of our two-stage numerical procedure, we did not use any knowledge of the dielectric constant of this prism. We have only used the fact that $\varepsilon_r = 1$ outside of this prism, see (6.1).

We have placed one dielectric inclusion inside of this prism. Inclusions were two wooden cubes, which we call below “Cube 1” and “Cube 2”. Sizes of their sides were 4 cm for Cube 1 and 6 cm for Cube 2. Note that only refractive indices $n = \sqrt{\varepsilon_r}$ rather than dielectric constants can be measured directly in experiments. The goal of the first stage was to reconstruct the refractive index of the inclusion and its location. The goal of the second stage was to reconstruct all three components of inclusions: refractive indices, shapes and locations. Since only one component of the electric field was measured, we have modeled the wave propagation process via the problem (8.2) with $\varepsilon_r(x) := c(x)$, where the domain $G \subset \mathbb{R}^3$ was a prism, which was bigger than the prism Ω , see (5.8) and section 5.4 in [11] for this domain. The function $f(t)$ in (8.2) was

$$f(t) = \begin{cases} \sin(\omega t), & t \in (0, 2\pi/\omega), \\ 0, & t > 2\pi/\omega, \end{cases}$$

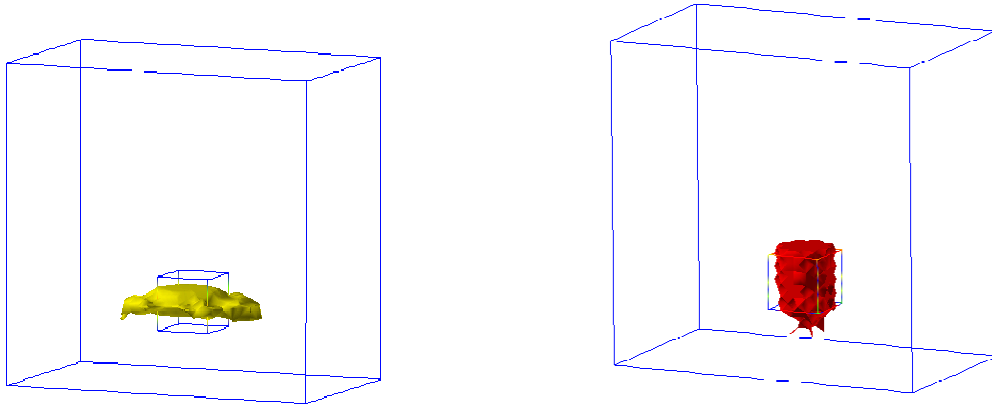
where $\omega = 14$ for Cube 1 and $\omega = 7$ for Cube 2 (see page 329 of [11] and page 26 of [15] for ω). It was only later, after the first author has conducted numerical simulations for solving the Maxwell equations [18], when we have realized that the choice of modeling by one PDE only was well justified. In our experiments, Cubes 1 and 2 were placed total in six different positions.

Table 8.1 summarizes results of blind study of the first stage of our two-stage numerical procedure. Because of the blind test requirement, direct measurements of refractive indices were performed by the conventional so-called “waveguide method” [44] *only after* computations of the first stage were done. Next, computational results were compared with measured ones. One can see that we had only a few percent difference with *a posteriori* directly measured refractive indices of both cubes. Furthermore, in five out of six cases this error was even less than the error in direct measurements.

We now focus on the results which we have obtained on the second stage of our two-stage numerical procedure when applying the adaptivity.

Test 2. The two stage numerical procedure for Case 1 of Table 8.1. Figure 8.6-a) displays the result of the first stage of the two-stage numerical procedure. One can see that although the refractive index $n = 1.97$ and location of the inclusion are accurately calculated, the shape is inaccurate. The image of Figure 8.6-a) was taken as the starting point for the adaptivity technique for refinement. The result of the second stage is presented on Figure 8.6-b). One can see that all three components of the inclusion are accurately reconstructed. In addition, the values of the function $\varepsilon_r(x) := c(x) = 1$ outside of the imaged inclusion are also accurately computed.

Test 3. The two stage numerical procedure for Case 6 of Table 8.1. Figures 8.7-a) and 8.7-b) display computational results for first and second stages, respectively. The rest of comments are the same



$$\text{a) } \max n_{glob} = \max \sqrt{\varepsilon_{r, glob}} = \max \sqrt{c_{glob}} = 1.97$$

$$\text{b) } \max n = \max \sqrt{\varepsilon_r} = \max \sqrt{c} = 2.05$$

Fig. 8.6: Case 1 of Table 8.1 was tested by the two-stage numerical procedure. a) The computational result of the first stage. Both location of the inclusion and refractive index $n_{glob} = 1.97$ are accurately reconstructed. However, the shape of the inclusion is not reconstructed accurately. b) The computational result of the second (refinement) stage. All three components of the inclusion are very accurately reconstructed: refractive index, location and shape. Also, values of the function $\varepsilon_r(x) := c(x) = 1$ outside of the imaged inclusion are computed very accurately. Original source: L. Beilina and M.V. Klibanov, Reconstruction of dielectrics from experimental data via a hybrid globally convergent/adaptive inverse algorithm, *Inverse Problems*, 26, 125009, doi:10.1088/0266-5611/26/12/125009, 2010. ©IOP Publishing. Reprinted with permission.

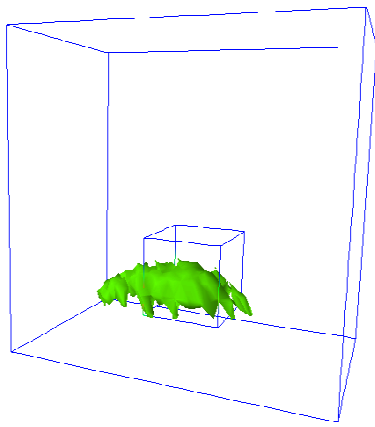
as ones for Test 2. Note that the shape is now reconstructed better than in Test 2. This can be heuristically explained as follows. The wavelength of our electromagnetic wave was $\mu = 3$ cm. Thus, the size of the side of Cube 1 is $4 \text{ cm} = 1.33\mu$. On the other hand, the size of the side of Cube 2 is $6 \text{ cm} = 2\mu$, which is larger.

Acknowledgments

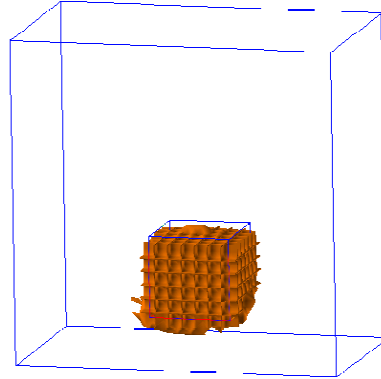
This research was supported by US Army Research Laboratory and US Army Research Office grant W911NF-11-1-0399, the Swedish Research Council, the Swedish Foundation for Strategic Research (SSF) in Gothenburg Mathematical Modelling Centre (GMMC) and by the Swedish Institute, Visby Program.

REFERENCES

- [1] M. Asadzadeh and L. Beilina, *A posteriori* error analysis in a globally convergent numerical method for a hyperbolic coefficient inverse problem, *Inverse Problems*, 26, 115007, 2010.
- [2] A.B. Bakushinskii and M.Yu. Kokurin, *Iterative Methods for Approximate Solution of Inverse Problems*, Springer, New York, 2004.
- [3] W. Bangerth and A. Joshi, Adaptive finite element methods for the solution of inverse problems in optical tomography, *Inverse Problems* 24, 034011, 2008.
- [4] R. Becker and R. Rannacher, An optimal control approach to a *posteriori* error estimation in finite element method, *Acta Numerica*, 10, 1-102, 2001.
- [5] L. Beilina, K. Samuelsson and K. Åhlander, Efficiency of a hybrid method for the wave equation. In *International Conference on Finite Element Methods*, Gakuto International Series Mathematical Sciences and Applications. Gakkotosho CO., LTD, 2001.
- [6] L. Beilina and C. Johnson, A hybrid FEM/FDM method for an inverse scattering problem. In *Numerical Mathematics and Advanced Applications - ENUMATH 2001*, Springer-Verlag, Berlin, 2001.
- [7] L. Beilina, Adaptive finite element/difference method for inverse elastic scattering waves, *Applied and Computational Mathematics*, 1, 158-174, 2002.



a) $\max n_{glob} = \max \sqrt{\varepsilon_{r,glob}} = \max \sqrt{c_{glob}} = 1.79$

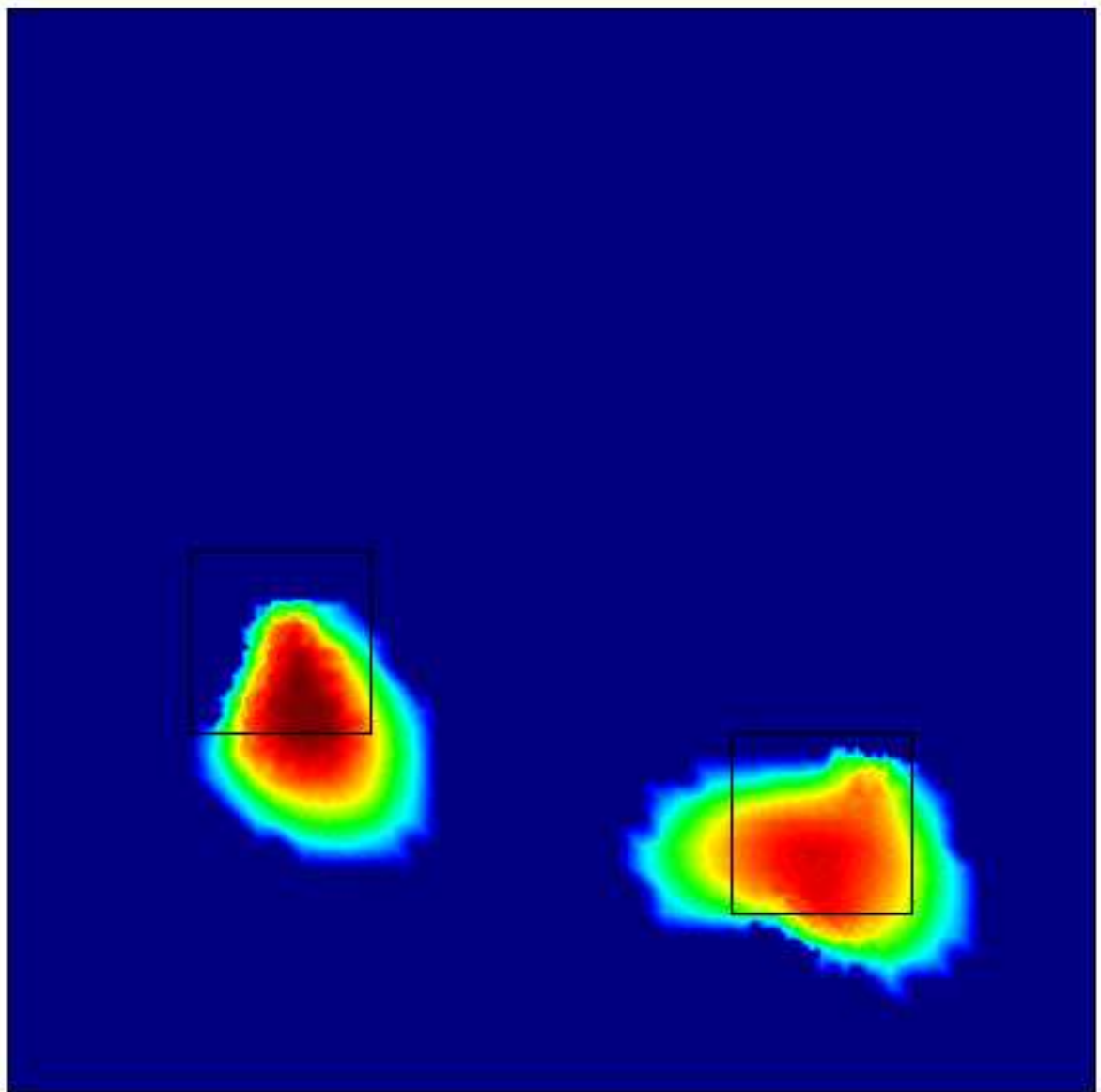


b) $\max n = \max \sqrt{\varepsilon_r} = \max \sqrt{c} = 1.73$

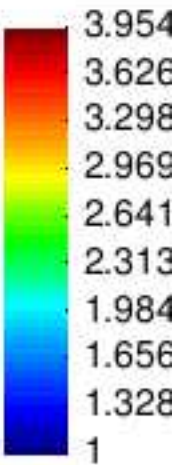
Fig. 8.7: Case 6 of Table 8.1 was tested for the two-stage numerical procedure. a) The computational result of the first stage. Both location of the inclusion and refractive index $n_{glob} = 1.79$ are accurately reconstructed. However, the shape of the inclusion is not reconstructed accurately. b) The computational result of the second (refinement) stage. All three components of the inclusion are accurately reconstructed: location, refractive index, and shape. In addition, values of the function $\varepsilon_r(x) := c(x) = 1$ outside of the imaged inclusion are computed accurately. Original source: L. Beilina and M.V. Klibanov, Reconstruction of dielectrics from experimental data via a hybrid globally convergent/adaptive inverse algorithm, *Inverse Problems*, 26, 125009, doi:10.1088/0266-5611/26/12/125009, 2010. ©IOP Publishing. Reprinted with permission.

- [8] L. Beilina and C. Johnson, *A posteriori* error estimation in computational inverse scattering, *Mathematical Models and Methods in Applied Sciences*, 15, 23-37, 2005.
- [9] L. Beilina and C. Clason, An adaptive hybrid FEM/FDM method for an inverse scattering problem in scanning acoustic microscopy, *SIAM J. Sci. Comp.*, 28, 382-402, 2006.
- [10] L. Beilina, Adaptive finite element method for a coefficient inverse problem for the Maxwell's system, *Applicable Analysis*, 90, 1461-1479, 2011.
- [11] L. Beilina and M.V. Klibanov, *Approximate Global Convergence and Adaptivity for Coefficient Inverse Problems*, Springer, New York, 2012.
- [12] L. Beilina and M.V. Klibanov, A globally convergent numerical method for a coefficient inverse problem, *SIAM J. Sci. Comp.*, 31, 478-509, 2008.
- [13] L. Beilina and M.V. Klibanov, Synthesis of global convergence and adaptivity for a hyperbolic coefficient inverse problem in 3D, *J. Inverse and Ill-posed Problems*, 18, 85-132, 2010.
- [14] L. Beilina and M.V. Klibanov, *A posteriori* error estimates for the adaptivity technique for the Tikhonov functional and global convergence for a coefficient inverse problem, *Inverse Problems*, 26, 045012, 2010.
- [15] L. Beilina and M.V. Klibanov, Reconstruction of dielectrics from experimental data via a hybrid globally convergent/adaptive inverse algorithm, *Inverse Problems*, 26, 125009, 2010.
- [16] L. Beilina, M.V. Klibanov and M.Yu. Kokurin, Adaptivity with relaxation for ill-posed problems and global convergence for a coefficient inverse problem, *Journal of Mathematical Sciences*, 167, 279-325, 2010.
- [17] L. Beilina and M.V. Klibanov, A new approximate mathematical model for global convergence for a coefficient inverse problem with backscattering data, *J. Inverse and Ill-Posed Problems*, 20, 2012, to appear.
- [18] L. Beilina, Energy estimates and numerical verification of the stabilized domain decomposition finite element/finite difference approach for the Maxwell's system in time domain, *Central European Journal of Mathematics*, accepted for publication; preprint is available online at <http://publications.lib.chalmers.se/publication/142368>.
- [19] A.L. Bukhgeim and M.V. Klibanov, Uniqueness in the large of a class of multidimensional inverse problems, *Soviet Math. Doklady*, 17, 244-247, 1981.
- [20] A.L. Bukhgeim, Carleman estimates for Volterra operators and uniqueness of inverse problems, in *Non-Classical Problems of Mathematical Physics*, pages 54-64, published by Computing Center of the Siberian Branch of Russian Academy of Science, Novosibirsk, 1981 (in Russian).
- [21] A.L. Bukhgeim, *Introduction in The Theory of Inverse Problems*, VSP, Utrecht, The Netherlands, 2000.
- [22] D. Colton and R. Kress, *Inverse Acoustic and Electromagnetic Scattering Theory*, Springer, New York, 1992.

- [23] H.W. Engl, M. Hanke and A. Neubauer, *Regularization of Inverse Problems*, Kluwer Academic Publishers, Boston, 2000.
- [24] B. Engquist and A. Majda, Absorbing boundary conditions for the numerical simulation of waves *Math. Comp.* 31, 629-651, 1977.
- [25] K. Eriksson, D. Estep and C. Johnson, *Calculus in Several Dimensions*, Springer, Berlin, 2004.
- [26] T. Feng, N. Yan and W. Liu, Adaptive finite element methods for the identification of distributed parameters in elliptic equation, *Advances in Computational Mathematics*, 29, 27-53, 2008.
- [27] S.I. Kabanikhin, *Inverse and Ill-Posed Problems. Theory and Applications*, De Gruyter, Berlin, 2012.
- [28] M. V. Klibanov, Uniqueness of solutions in the 'large' of some multidimensional inverse problems, in *Non-Classical Problems of Mathematical Physics*, pages 101-114, 1981, published by Computing Center of the Siberian Branch of the Russian Academy of Science, Novosibirsk (in Russian).
- [29] M. V. Klibanov, Inverse problems in the 'large' and Carleman bounds, *Differential Equations*, 20, 755-760, 1984.
- [30] M. V. Klibanov, Inverse problems and Carleman estimates, *Inverse Problems*, 8, 575-596, 1992.
- [31] M. V. Klibanov and A. Timonov, *Carleman Estimates for Coefficient Inverse Problems and Numerical Applications*, VSP, Utrecht, 2004.
- [32] M. V. Klibanov, M. A. Fiddy, L. Beilina, N. Pantong and J. Schenk, Picosecond scale experimental verification of a globally convergent numerical method for a coefficient inverse problem, *Inverse Problems*, 26, 045003, 2010.
- [33] M.V. Klibanov, A.B. Bakushinskii and L. Beilina, Why a minimizer of the Tikhonov functional is closer to the exact solution than the first guess, *J. Inverse and Ill-Posed Problems*, 19, 83-105, 2011.
- [34] M.V. Klibanov, Uniqueness of an inverse problem with single measurement data generated by a plane wave in partial finite differences, *Inverse Problems*, 27, 115005, 2011.
- [35] M.V. Klibanov, Carleman estimates for global uniqueness, stability and numerical methods for coefficient inverse problems, *arXiv* : 1210.1780v1 [math-ph].
- [36] N. Koshev and L. Beilina, A posteriori error estimates for Fredholm integral equations of the first kind, accepted for publication in *Springer Proceedings in Mathematics*, Springer, 2012.
- [37] A. V. Kuzhuget, L. Beilina and M. V. Klibanov, Approximate global convergence and quasi-reversibility for a coefficient inverse problem with backscattered data, *Journal of Mathematical Sciences*, 181, 19-49, 2012.
- [38] A.V. Kuzhuget, L. Beilina, M.V. Klibanov, A. Sullivan, L. Nguyen and M.A. Fiddy, Blind experimental data collected in the field and an approximately globally convergent inverse algorithm, *Inverse Problems*, 28, 095007, 2012.
- [39] O. A. Ladyzhenskaya, *Boundary Value Problems of Mathematical Physics*, Springer Verlag, Berlin, 1985.
- [40] J. Li, J. Xie and J. Zou, An adaptive finite element reconstruction of distributed fluxes, *Inverse Problems*, 27, 075009, 2011.
- [41] M. Minoux, *Mathematical Programming: Theory and Algorithms*, Wiley and Sons, Chichester, 1986.
- [42] J. Nocedal, Updating quasi-Newton matrices with limited storage, *Mathematics of Comp.*, 35, 773-782, 1991.
- [43] R. Ramlau, TIGRA- an iterative algorithm for regularizing nonlinear ill-posed problems, *Inverse Problems*, 19, 433-465, 2003.
- [44] J.R. Reitz, F.J. Milford, and R.W. Christy, *Foundations of Electromagnetic Theory*, Reading, Mass., Addison-Wesley, 1980.
- [45] A. N. Tikhonov and V. Ya. Arsenin, *Solutions of Ill-Posed Problems*, Winston and Sons, Washington, DC, 1977.
- [46] A.N. Tikhonov, A.V. Goncharsky, V.V. Stepanov and A.G. Yagola, *Numerical Methods for the Solution of Ill-Posed Problems*, Kluwer, London, 1995.
- [47] The software package WavES, available at <http://waves24.com>.
- [48] M. Yamamoto, Carleman estimates for parabolic equations and applications, *Inverse Problems*, 25, 123013, 2009.



Scalar result



y
z x

step 15

Contour Fill of Scalar result.

